Structural Reliability and Stochastic Finite Element Methods: State-of-the-art Review and Evidence-based Comparison

Muhannad Aldosary [*], Jinsheng Wang [*], Chenfeng Li [*, †]

Zienkiewicz Centre for Computational Engineering, Swansea University, Swansea,U.K.

Enger Safety Research Institute, Swansea University, Swansea, U.K.

Abstract

Purpose: Uncertainties are widely encountered in engineering practice, arising from such diverse sources as heterogeneity of materials, variability in measurement, lack of data, and ambiguity in knowledge etc. Academia and industries have long been researching for Uncertainty Quantification (UQ) methods to quantitatively account for the effects of various input uncertainties on the system response. Despite the rich literature of relevant research, UQ is not an easy subject for novice researchers / practitioners, where many different methods and techniques coexist with inconsistent input/output requirements and analysis schemes.

Design/methodology/approach: This confusing status significantly hampers the research progress and practical application of UQ methods in engineering. In the context of engineering analysis, the research efforts of UQ are most focused in two largely separate research fields: Structural Reliability Analysis (SRA) and Stochastic Finite Element Method (SFEM). This paper provides a state-of-the-art review of SRA and SFEM, covering both technology and application aspects. Moreover, unlike standard survey papers that focus primarily on description and explanation, a thorough and rigorous comparative study is performed to test all UQ methods reviewed in the paper on a common set of reprehensive examples.

Findings: Critical opinions and concluding remarks are drawn from the rigorous comparative study, providing objective evidence-based information for further research as well as practical applications.

Keywords: *structural reliability, stochastic finite element method, uncertainty quantification, uncertainty propagation, random field, random variable, surrogate model.*

1 Introduction

The analysis and design of complex structures or engineering systems rely heavily on predictions from numerical models (e.g. finite element analysis), while the accuracy of the numerical results depends on the proximity between the digital representation and the real-world system. The feasibility, applicability, and confidence level of numerical models are frequently challenged by the presence of various evitable uncertainties in engineering structures and systems. This has motivated the research of Uncertainty Quantification (UQ) in engineering analysis, which has historically been pursued in two largely separate research fields: Structural Reliability Analysis (SRA) and Stochastic Finite Element Method (SFEM).

SRA and the associated risk assessment have long been established in the civil engineering community, where the earliest research work can be dated back to over half a century ago. Over the years, SRA has gradually grown from an academic research topic to a more applied field emphasising applications in such critical structures as dams, tunnels, nuclear stations, and offshore structures etc. It aims to provide a rational framework to address uncertainties in structural analysis such that design can be more objective and less dependent on ideal assumptions. Despite the continuous progress in SRA, the estimation of structural reliability remains a challenging problem for structural engineers. The SRA theory is formulated around a core concept, namely the probability of failure:

$$P_f = Prob[g(\boldsymbol{x}) \leq 0] = \int_{g(\boldsymbol{x})\leq 0} f_{\boldsymbol{X}}(\boldsymbol{x})\, d\boldsymbol{x} \tag{1}$$

where $f_{\boldsymbol{X}}(\boldsymbol{x})$ is the joint Probability Density Function (PDF) of random vector $\boldsymbol{X}$, and $g(\boldsymbol{x})$ is the limit state function (also known as the performance function) with $g(\boldsymbol{x}) \leq 0$ denoting the failure domain and $g(\boldsymbol{x}) > 0$

[*] E-mails: 716663@swansea.ac.uk; 844051@swansea.ac.uk; c.f.li@swansea.ac.uk
[†] Corresponding author

the safe domain. The definition of P_f is simple, but its exact evaluation through direct integration is often intractable for practical problems, where the dimension of the integral is usually high and the limit state surface has complicated shape and topology. Moreover, direct integration is completely unfeasible when the joint PDF $f_{\boldsymbol{X}}(\boldsymbol{x})$ is unknown. Difficulties in computing the failure probability P_f has led to the development of various SRA methods, such as first and second order reliability methods, Monte Carlo simulation, important sampling, to name a few.

SFEM is another major UQ research field in engineering analysis. The development of the standard FEM started from the 1950s, and during the past few decades it has become the dominant engineering simulation tool for analysing materials, structures and subsystems in almost all engineering sectors, especially in automotive, aerospace, manufacturing and civil engineering industries. As a deterministic analysis tool, all input variables in the standard FEM must be uniquely specified and the output solutions are also uniquely resolved in the form of constant values. To account for the various uncertainties encountered in engineering practice, researchers have been trying to extend the standard FEM into SFEM by incorporating random variables into the mathematical and computational formulations. The simulation capacity of SFEM has been growing steadily over the past decade, as a result of continuous algorithm development and growth in computing power. In the wider context, SFEM aims to provide numerical solutions to stochastic partial differential equations, and it has been applied in very diverse engineering topics including solid materials, structures, fluid flow, acoustics, and heat transfer problems etc.

The aim of this study is to present a comprehensive and critical review of all existing SRA and SFEM approaches, with a particular emphasis on the potential of practical applications. The advantages and drawbacks of individual methods are elaborated through a rigorous comparative study, which provides objective evidence-based information for the feasibility and performance of different methods with respect to specific applications. The rest of the paper is organized as follows: the methods for transformation and discretization of random variables and fields are introduced in Section 2; technical summaries of various SRA and SFEM approaches are presented in Section 3 and Section 4, respectively; based on a set of carefully designed representative examples, a rigorous comparative study is presented in Section 5, covering all SRA and SFEM approaches reviewed in the paper; Section 6 draws the concluding remarks from the unbiased comparative study.

2 Transformation and discretization techniques for random variables and random fields

Uncertainties in engineering analysis are often associated with material properties (e.g. mass density, elasticity, permeability and damping factors etc.), geometry and boundary conditions of the concerned structure, and they are commonly modelled as discrete random variables or continuous random fields. For both SRA and SFEM, it is often essential and beneficial to perform transformation between different types of random variables and establish discretization of random fields. A random field $f(\boldsymbol{x},\theta)$ can be defined as a curve in the probability space $(\Theta,\Omega,\mathrm{P})$, containing a collection of random variables indexed by a parameter $\boldsymbol{x}\in\Omega$, where Ω is a subset of $\mathbb{R}^d$ defined by the system geometry. For a given point $\boldsymbol{x}_0$, $f(\boldsymbol{x}_0,\theta)$ is a random variable, while for a given event θ_0 , $f(\boldsymbol{x},\theta_0)$ is a realization of the random field [1, 2]. The random field $f(\boldsymbol{x},\theta)$ can be univariate or multivariate depending on whether the quantity $f(\boldsymbol{x})$ attached to the point $\boldsymbol{x}$ is a random variable or a random vector. Also, $f(\boldsymbol{x},\theta)$ can be one- or multi- dimensional depending on the dimensionality of Ω. Different mathematical and computational methods have been developed for the transformation and discretization task, and a brief summary is provided below.

2.1 Radom variable transformation

Random variables quantified directly from practical observations can be of various probabilistic distributions, whose representation and statistical computation can be very different. To ease the task in SRA and SFEM, it is often beneficial to transform the original random variables from the physical space to the standard normal space for mathematical and computational processing. A number of transformation techniques have been developed for the task, among which Rosenblatt transformation and Nataf transformation are two most widely used approaches [3, 4]. Let $\boldsymbol{X}$ denote a random vector defined in the physical space, the transformation of $\boldsymbol{X}$ is defined as:

$$\boldsymbol{U}=T(\boldsymbol{X}) \tag{2}$$

where $\boldsymbol{U}$ is a standard Gaussian random vector with zero mean and unit covariance matrix. If the joint Cumulative Distribution Function (CDF) of $\boldsymbol{X}$ is known, Rosenblatt transformation can be applied [3]:

$$\begin{aligned} T_1 &= \Phi^{-1}\left[F_{X_1}(x_1)\right] \\ T_2 &= \Phi^{-1}\left[F_{X_2}(x_2|x_1)\right] \\ &\cdots \\ T_M &= \Phi^{-1}\left[F_{X_M}(x_M|x_1,\ldots,x_{M-1})\right] \end{aligned} \tag{3}$$

where$F_{X_i}(x_i|x_1,\ldots,x_{i-1})$is the conditional distribution function and Φ is the standard normal CDF. However, in practical problems, the probabilistic information of random variables is usually limited to the marginal distribution and the correlation coefficients. For these cases, Rosenblatt transformation is unfeasible and Nataf transformation is suggested by Der Kiureghian and Liu [4]. Specifically, the random vector $\boldsymbol{Z}$ is obtained by using the marginal PDF of X_i:

$$Z_i = \Phi^{-1}\left[F_{X_i}(x_i)\right], \quad i = 1,\ldots,M \tag{4}$$

where $\boldsymbol{Z}$ is a Gaussian random vector with the correlation matrix $\boldsymbol{R}_0$, and $F_{X_i}(x_i)$ is the marginal distribution function. The joint PDF of $\boldsymbol{X}$ is determined by using the inverse transformation of Eqn. (4) as:

$$f_{\boldsymbol{X}}(\boldsymbol{x}) = f_{X_1}(x_1)\ldots f_{X_n}(x_n)\frac{\varphi_n(\boldsymbol{z},\boldsymbol{R}_0)}{\varphi(z_1)\ldots\varphi(z_n)} \tag{5}$$

The unknown correlation matrix $\boldsymbol{R}_0$ can be obtained by solving the following implicit equation:

$$\rho_{ij} = \iint_{-\infty}^{+\infty}\left(\frac{x_i-\mu_i}{\sigma_i}\right)\left(\frac{x_j-\mu_j}{\sigma_j}\right)\varphi_2(z_i,z_j,\rho_{0,ij})\,dz_i dz_j \tag{6}$$

for which semi-empirical formulations have been adopted to simplify the calculation [4]. After defining the correlation matrix $\boldsymbol{R}_0$ of the vector $\boldsymbol{Z}$, the transformation to the standard space can be expressed as:

$$\mathrm{T}(\mathbf{X}) = \mathbf{L}_0^{-1}.\mathbf{Z} = \mathbf{L}_0^{-1}.\{\Phi^{-1}\left[\mathrm{F}_{\mathrm{X}_1}(x_1)\right],\ldots,\Phi^{-1}\left[\mathrm{F}_{\mathrm{X}_n}(x_n)\right]\}^{\mathrm{T}} \tag{7}$$

where the transformation matrix $\boldsymbol{L}_0$ is determined by the Cholesky decomposition of $\boldsymbol{R}_0$, i.e. $\boldsymbol{R}_0 = \boldsymbol{L}_0.\boldsymbol{L}_0^T$.

2.2 Radom field discretization

Introduced by Ghanem [5-7], the Karhunen-Loève (K-L) expansion is arguably the most widely used tool for random field discretization, especially for uncertainties associated with input parameters. The K-L expansion represents the random field as a linear combination of orthogonal basis terms, which are determined by solving the Fredholm integral equation:

$$\int_\Omega R(\boldsymbol{x},\boldsymbol{x}')\,\varphi_i(\boldsymbol{x}')\,d\Omega_{\boldsymbol{x}'} = \lambda_i\,\varphi_i(\boldsymbol{x}) \qquad \forall\ i = 1,\ldots. \tag{8}$$

where the kernel autocovariance function $R(\boldsymbol{x},\boldsymbol{x}')$ is bounded, symmetric and positive definite. Thus all eigenvalues λ_i are real and positive, and the deterministic functions $\varphi_i(\boldsymbol{x})$ form a complete orthogonal basis of Hilbert spaces $\mathcal{L}^2(\Omega)$. The K-L expansion of the random field $f(\boldsymbol{x},\theta)$ is:

$$f(\boldsymbol{x},\theta) = \mu(\boldsymbol{x}) + \sum_{i=1}^{\infty}\sqrt{\lambda_i}\,\xi_i(\theta)\,\phi_i(\boldsymbol{x}) \tag{9}$$

where $\{\xi_i(\theta), i = 1,\ldots\}$ are a set of uncorrelated random variables, and they become independent Gaussian random variables if $f(\boldsymbol{x},\theta)$ is a Gaussian field. In practice, only a finite number of terms in the K-L expansion are used, where the truncation is performed after sorting the eigenvalues λ_i in a descending order.

Analytical solutions to the K-L expansion are available for simple geometries and special forms of the autocovariance function. However, for more general cases, numerical solutions to Eqn. (8) are required to obtain the corresponding K-L expansion. These numerical solutions usually have a high computational cost, while the obtained approximations are rarely optimal. The effectiveness of the K-L expansion is affected by the accuracy of the eigenpair λ_i and $\varphi_i(x)$ [8], for which several effective solution methods to the Fredholm integral equation (8) have been reported in the literature [9, 10].

To overcome the computational difficulties in the K-L expansion of random fields, Li et al. [11-14] proposed the Fourier-Karhunen-Loève (F-K-L) expansion, which is based on the spectral representation theory

of wide-sense stationary stochastic fields and the standard dimensionality reduction technology of principal component analysis. The F-K-L expansion is independent from the detailed shape of the random structure, and is a completely meshfree scheme therefore avoiding the mesh convergence and mesh sensitivity problems often encountered in the mesh-based discretization schemes. In all our experiments where the discretization of a continuous random field is required, the F-K-L expansion has exhibited a much higher accuracy and efficiency over mesh-based discretization schemes. The superior accuracy and efficiency of the F-K-L expansion is due to the harmonic essence of wide-sense stationary stochastic fields.

3 Structural reliability analysis

As outlined in Section 1, the SRA theory is centered on the concept of failure probability P_f, which is essentially a multi-dimensional integral over the failure domain determined by the limit state function. The computational cost to calculate the probability of failure can be prohibitive, especially for evaluating small P_f values, which is almost always the case in the practical world. Various approximation methods have been developed to evaluate the failure probability, forming a rich literature of SRA. These SRA methods can be broadly classified into three categories: Taylor-series based approaches such as the First Order Reliability Analysis Method (FORM) and the Second Order Reliability Analysis Method (SORM), simulation based methods such as Monte Carlo simulation and its variants, and surrogate methods such as the Response Surface Method (RSM) and the Kriging meta-model. A brief summary of various SRA approaches are presented in the following subsections.

3.1 FORM and SORM

As one of the oldest SRA method, FORM applies the first-order Taylor expansion to linearize the limit state surface in the standard normal space at the so-call Most Probable Point (MPP) $\boldsymbol{U}^*$, which has the highest likelihood among all points in the failure region [3, 15, 16]:

$$g(\boldsymbol{X}) \equiv g(\boldsymbol{U}) = g(\boldsymbol{U}^*) + \boldsymbol{\nabla} g(\boldsymbol{U}^*)^T(\boldsymbol{U} - \boldsymbol{U}^*) \tag{10}$$

where $\boldsymbol{\nabla} g(\boldsymbol{U}^*)$ is the gradient vector at $\boldsymbol{U}^*$. The reliability index β is defined as the shortest distance from the origin to the failure surface, and the failure probability is approximated by $P_f = \Phi(-\beta)$. Following the definition of the reliability index, MPP can be obtained from a constrained optimization problem in the standard normal space as:

$$\boldsymbol{U}^* = argmin\{Q(\boldsymbol{U}) = \tfrac{1}{2}\|\boldsymbol{U}\|^2 \Big|\ g(\boldsymbol{U}) \le 0\} \tag{11}$$

A number of optimization algorithms are available to solve this problem, interested readers can refer to [16-18] for more information.

To further improve the accuracy of FORM, a second-order Taylor expansion at MPP can be adopted to approximate the limit state surface and this leads to the formulation of SORM [19-23]. Specifically, the limit state surface is approximated by a quadratic surface in the standard normal space:

$$g(\boldsymbol{U}) = \boldsymbol{\alpha}^T\boldsymbol{U}^* - \boldsymbol{\alpha}^T\boldsymbol{U} + \tfrac{1}{2}(\boldsymbol{U} - \boldsymbol{U}^*)^T\boldsymbol{B}(\boldsymbol{U} - \boldsymbol{U}^*) \tag{12}$$

where $\boldsymbol{\alpha} = \frac{\boldsymbol{\nabla} g(\boldsymbol{U}^*)}{|\boldsymbol{\nabla} g(\boldsymbol{U}^*)|}$, $\boldsymbol{B} = \frac{\boldsymbol{\nabla^2} g(\boldsymbol{U}^*)}{|\boldsymbol{\nabla} g(\boldsymbol{U}^*)|}$, $\boldsymbol{\nabla^2} g(\boldsymbol{U}^*)$ is the Hessian evaluated at the MPP. Several formulas are available to obtain the failure probability in the context of SORM, among which an asymptotic formula proposed by Breitung is widely used [19]:

$$P_f = \Phi(-\beta_{FORM}) \prod_{j=1}^{N-1}(1 + \beta_{FORM}\, k_j)^{-1/2} \tag{13}$$

where $k_j,\ j = 1, \dots, N-1$ are principal curvatures at the MPP. Attempts to improve the efficiency and accuracy of SORM are still continuing [24-28].

3.2 Simulation based methods

If the limit state function is highly nonlinear, large errors may be introduced into the failure probability calculation when using FORM or SORM, as the limit state surface is approximated only with lower-order

Taylor expansions. To achieve better accuracy in these cases, an alternative approach is the simulation based SRA methods, which generate samples of the limit state function with FE simulation and directly estimate the failure probability through numerical integration.

3.2.1 Monte Carlo simulation

The Monte Carlo Simulation (MCS) method is arguably the most robust and versatile SRA approach, albeit at high computational cost [29]. The failure probability in MCS is defined as the ratio of the number of samples in the failure domain to the total number of samples:

$$\hat{P}_f = \frac{N_f}{N} = \frac{1}{N}\sum_{i=1}^{N} I[g_i(\boldsymbol{x}) \leq 0] \tag{14}$$

where the sampling points $\boldsymbol{x}$ are generated according the PDF $f_{\boldsymbol{X}}(\boldsymbol{x})$, N_f is the number of sampling points such that $g(\boldsymbol{x}) \leq 0$, N is the total number of sampling points, $g_i(\boldsymbol{x})$ is the i^{th} realization of the limit state surface; $I[g(\boldsymbol{x})]$ is an indicator function taking values of unity if $g(\boldsymbol{x}) \leq 0$ and zero otherwise.

With a convergence rate of $O(\frac{1}{\sqrt{N}})$, the computational cost of MCS can be prohibitively high for complex problems, especially when time consuming numerical codes such as finite element analysis are involved in sample generation. In order to address this problem, many variance reduction techniques such as Importance Sampling (IS), Directional Sampling (DS), Latin Hypercube Sampling (LHS), Line Sampling (LS) and Subset Simulation (SS), have been proposed to conduct failure probability estimation with a reduced computational cost. These methods are briefly recapped in the following subsections, while more details are referred to the original papers and summary textbooks where appropriate.

3.2.2 Importance sampling

The key idea of Importance Sampling (IS) is to distribute the sampling points in the region of the greatest importance such that the failure probability evaluation can be accelerated. Specifically, Eqn. (1) is reformulated as:

$$P_f = \int_{g(\boldsymbol{x})\leq 0} \frac{f_X(\boldsymbol{x})}{h_{\boldsymbol{X}}(\boldsymbol{x})}\, h_{\boldsymbol{X}}(\boldsymbol{x})d\boldsymbol{x} \tag{15}$$

where $h_{\boldsymbol{X}}(\boldsymbol{x})$ is the IS density function. Hence, the probability of failure can be approximated as:

$$P_f = \frac{1}{N}\sum_{j=1}^{N} I(\boldsymbol{x}_j)\frac{f_X(\boldsymbol{x}_j)}{h_X(\boldsymbol{x}_j)} \tag{16}$$

where the sampling points $\boldsymbol{x}_j, j = 1, \dots, N$ are generated according to the distribution $h_{\boldsymbol{X}}$ instead of $f_{\boldsymbol{X}}$. The effectiveness of IS depends on the selection of an appropriate $h_{\boldsymbol{X}}(\boldsymbol{x})$ such that the probabilistic sampling in Eqn. (16) can be prioritized for the region of the greatest importance, therefore achieving a better convergence rate. Although there is no general conclusion on the choice of $h_{\boldsymbol{X}}(\boldsymbol{x})$ [30-32], it has been argued that the MPP and its neighbourhood can be a good option for the region of the greatest importance unless additional information on the limit state function and the failure probability are available. The MPP can be identified by FORM. However, unlike FORM or SORM, the IS estimation is not sensitive to the exact position of MPP, therefore it does not need to be determined up to a high accuracy.

It is well known that the MPP and its neighbourhood do not always describe the most 'important' region of the failure domain, especially in high dimensional space. An alternative approach is to place the sampling points inside the failure domain in order to create the optimal importance sampling density function. In the earlier attempts, a rejection sampling scheme following the original PDF $f_{\boldsymbol{X}}(\boldsymbol{x})$ was adopted [33], but this is extremely inefficient in cases where the failure probability is small. To improve the efficiency, a Markov chain metropolis algorithm was introduced, and points $\boldsymbol{x}_i$ with a distribution of h_{opt} can be obtained as intermediate states of an irreducible Markov chain [34, 35]. The initial point $\boldsymbol{x}_0$ can be selected either by rejection sampling or using engineering assessment. Subsequently, a kernel sampling density estimator is created using N_v points $\boldsymbol{x}_i$ obtained by the Markov chain:

$$k(\boldsymbol{x}) = \frac{1}{N_v}\sum_{i=1}^{N_v} \frac{1}{(w\boldsymbol{\lambda}_i)^M} K\left(\frac{\boldsymbol{x}-\boldsymbol{x}_i}{w\boldsymbol{\lambda}_i}\right) \tag{17}$$

where w is the window width, $\boldsymbol{\lambda}_i$ is the local bandwidth factor, M is dimensional space and K is the kernel PDF, often set as the multivariate normal. The density $k(\boldsymbol{x})$ is employed as the importance sampling density to estimate P_f based on Eqn. (16). Several methods have been developed to adjust w and $\boldsymbol{\lambda}_i$ so that the estimate obtained Eqn. (17) is optimal [35, 36]. There are many other further improvements following the IS approach, and some of these variants rely on the concept of adaptive sampling [37, 38], which has shown promising results in evaluating the failure probability.

3.2.3 Directional sampling

The Directional Sampling (DS) method was originally proposed to evaluate the multivariate distribution function, and has been adopted to calculate the probability of failure in the $\boldsymbol{U}$-space for general structural reliability problems [39-42]. The DS method generates uniformly distributed direction vectors and along each direction a one-dimensional integration is performed. The reference [43] used a series of hyperspherical segments, whose radii follow a Chi-square χ^2 distribution, to investigate the actual limit state surface in the standard normal space. Practically, a sequence of N random direction vectors $\boldsymbol{a}^{(j)} = \frac{\boldsymbol{u}^{(j)}}{\|\boldsymbol{u}^{(j)}\|}, j = 1, \dots, N$ are generated first, then $r_j = \{r | g(r\boldsymbol{a}^{(j)}) = 0\}$ are found iteratively. Finally the sum of the failure probabilities associated with those segments gives the approximated probability of failure:

$$P_f = \frac{1}{N}\sum_{j=1}^{N}[1 - \chi_M^2(r_j^2)] \tag{18}$$

where χ_M^2 is the chi-square CDF with M d.o.f.. The DS method is relatively more efficient compared to other Monte Carlo simulation approaches, but its performance drops dramatically when the limit state surface is highly nonlinear. As the prior knowledge of the limit state is rarely available, search-based importance sampling has been proposed, which increases the cost of computation. Moreover, the randomly generated samples in DS may not be optimal, and several new approaches have been proposed to better identify integration directions (e.g. spherical t-design, spiral points, and Fekete points) [44]. Once determined, the DS directions can be readily reused for calculations of other probabilistic integrations. The efficiency of DS was significantly improved recently [45] by utilizing deterministic point sets to preserve the underlying joint probability distribution and by employing neural networks to focus the simulation effort in the significant regions.

3.2.4 Subset simulation

Subset Simulation (SS) [46, 47] expresses the failure probability as a product of a series of conditional probabilities for some chosen intermediate failure events, whose estimations are cheaper than evaluating directly the overall failure probability. The conditional probabilities are obtained from Markov Chains Monte Carlo (MCMC) simulation, based on a modified Metropolis-Hastings algorithm. The efficiency and accuracy of SS depend on the ability of the MCMC algorithm to accurately estimate the conditional probabilities with a minimum number of samples. The idea of SS has attracted wider attention: it was suggested in [48, 49] to split the trajectory in order to increase the acceptance rate of a candidate sample; a spherical SS for high dimensional problems was proposed in [50]; an optimal scaling technique was developed in [51] for the modified Metroplis-Hasting algorithm, with a theoretical analysis for the optimal value of the conditional failure probability. SS methods have been widely applied in various UQ problems, including structures subjected to uncertain earthquake ground motions [46-48, 50, 52, 53], aerospace engineering [54], geotechnical engineering [55] and nuclear engineering [56].

The failure of a practical structure $F = \{g(\boldsymbol{x}) \leq 0\}$ is usually a rare event, corresponding to a small failure region in the random parameter space. Let $F_1 \supset F_2 \supset \cdots \supset F_m = F$ denote a decreasing sequence of failure events, which are defined as $F_i = \{g(\boldsymbol{x}) \leq y_i\}$ with decreasing y_i values for the limit state surface and $y_m = 0$. Following the definition of failure probability, it can be calculated as [46]:

$$P_f = P(F) = P(F_m) = P(F_m|F_{m-1})P(F_{m-1}) = \cdots = P(F_1)\prod_{i=2}^{m} P(F_i|F_{i-1}) \tag{19}$$

Although the original failure probability P_f may be small, by choosing the appropriate intermediate failure events $\{F_i, i = 1, \dots, m\}$ it is possible to evaluate more efficiently the associated conditional probabilities in

Eqn. (19). To calculate the probability of failure from Eqn. (19), one needs to compute the probabilities $P(F_1)$ and $\{P(F_i|F_{i-1}): i = 2, \dots, m\}$. The first threshold y_1 is obtained by a crude MCS, such that $P(F_1) = p_0$, where p_0 is target probability for each subset step. For further thresholds, new sampling points corresponding to the conditional events $(F_i|F_{i-1})$ are obtained from MCMC using on a modified Metropolis-Hastings algorithm [46, 51], and the conditional probability $P(F_j|F_{j-1})$ can be estimated as:

$$P_j = P(F_j|F_{j-1}) \approx \frac{1}{N}\sum_{i=1}^{N} I_{F_j}(g(\boldsymbol{x}_i)) \tag{20}$$

Finally, the failure probability of the target event is calculated as as $P_f = \prod_{j=1}^{m} P_j$.

3.2.5 Latin hypercube sampling

The Latin Hypercube Sampling (LHS) method is a popular tool to improve the efficiency of crude Monte Carlo sampling. The LHS was originally proposed in [57] and has been further developed for different purposes by many researchers [58-62]. The LHS is very efficient for estimating mean values and standard deviations [62], but it is only slightly more efficient than the crude MCS for estimating small probabilities [63]. Recently, some studies demonstrated the robustness of the LHS and the accuracy of the estimated probability of failure for both regular and irregular configurations [64] . LHS aims to spread the sample points more evenly across the domain, therefore with the same sample size it is more stable and more accurate than the estimation produced by MC sampling [65]. The main idea is a stratification of the probability distribution by dividing the CDF curve into equal intervals and then choosing one sample randomly inside each stratification. Taking the two-dimensional sample space as an example, a square grid is a Latin square if and only if there is only one sample in each row and each column. LHS extends this concept to arbitrary dimensions, whereby each sample is the only one in each dimension-aligned hyperplane including it. Unlike MCS, where the generation of later samples are completely independent from the early samples, the LHS requires to remember the history of sample generation such that its later samples do not overlap in the hyperplane of the early samples. It is worth to mention that even though the marginal distribution of each variable is efficiently represented, there is a risk that some spurious correlation will appear [65]. The correlation between random variables can be introduced during the LHS process that rearranges the samples to form pairs with desired correlation level, which is known as rank correlation. LHS with rank correlation technique is effective to generate sampling matrix with correlation structure rather close to the target correlation matrix [66]. Reference [67] applies LHS with Cholesky decomposition to minimize the correlation between samples of random variables in probabilistic space. Several authors have improved LHS by determining optimal pairings that either enhance space-filling or reduce spurious correlation (increasing orthogonality) [64].

It is worth to note that other types of space-filling random sampling strategies such as Sobol series and Halton sequences [68] can also be used for structural reliability analysis.

3.3 Surrogate methods

In the aforementioned SRA methods, FE structural analysis is performed in every iteration of FORM/SORM or is required for every sample solution using the simulation based approach, which can be extremely time-consuming for complex structures. To reduce the computational cost associated with the FE simulation, an alternative approach is to approximate the actual limit state function with a surrogate model (also called meta-model) that is of a simpler form, after which the probability of failure can be efficiently estimated from the surrogate without resolving the actual limit function using FE simulation.

3.3.1 Response surface method

The Response Surface Method (RSM) [69-71] fits and identifies an approximate response surface model from input and output data collected from experimental / numerical studies, such that the actual limit state function $g(\boldsymbol{x})$ can be replaced with a simple function (often polynomial) $\hat{g}(\boldsymbol{x})$ for fast evaluation of the failure probability. In practice, quadratic functions with or without cross terms are often used to approximate the response surface:

$$g(\boldsymbol{x}) \approx \hat{g}(\boldsymbol{x}) = a_0 + \sum_{i=1}^{M} a_i x_i + \sum_{i=1}^{M} a_{ii} {x_i}^2 + \sum_{i=1}^{M}\sum_{j=1, j\neq i}^{M} a_{ij}\, x_i . x_j \tag{21}$$

where $\boldsymbol{a} = \{a_0, a_i, a_{ii}, a_{ij}\}$ are unknown coefficients and M denotes the number of random variables. The unknown polynomial coefficients $\{\boldsymbol{a}\}$ are determined by the least square regression technique using a sufficient number of experimental points. After constructing the response surface $\hat{g}(\boldsymbol{x})$, the reliability analysis can be performed on $\hat{g}(\boldsymbol{x})$ instead of the actual limit state function $g(\boldsymbol{x})$.

A number of design schemes are available to select the experimental points for construction of the approximate response surface, among which the central composite design is a well-known approach. However, this scheme requires $N = 2^n + 2n + 1$ evaluations of the exact limit state function, where the computational cost will be tremendous for large-scale structures with a large number of random variables. To reduce the number of fitting points, an adaptive interpolation scheme was proposed in [72], where a new centre point $\boldsymbol{x}_M$ for interpolation is chosen on a straight line from the mean vector $\boldsymbol{x}$ to the design point $\boldsymbol{x}^*$ obtained from the first constructed response surface:

$$\boldsymbol{x}_M = \boldsymbol{\mu}_{\boldsymbol{X}} + (\boldsymbol{x}^* - \boldsymbol{\mu}_{\boldsymbol{X}}) \frac{g(\boldsymbol{\mu}_{\boldsymbol{X}})}{g(\boldsymbol{\mu}_{\boldsymbol{X}}) - g(\boldsymbol{x}^*)} \tag{22}$$

This adaptive interpolation scheme ensures that the new center point is closer to the exact limit surface $g(\boldsymbol{x}) = 0$. The RSM has been continuously improved over the years, and the improvements include the adaptive iteration procedure [73], the gradient projection method to select sampling points [74], the coupled RSM and moment method [75], the adoption of the moving least-squares method for better response surface fitting [76], the use of exponential response surface [77], the artificial neural network based RSM and the support vector machine based RSM [78-81], among others.

3.3.2 Kriging

Kriging (also known as Gaussian process modelling) is another popular meta-modelling technique that is widely reported in the structural reliability and SFEM literature. Kriging was originally developed for geostatistics in the 50s and 60s by Krige and then by Matheron [82], and the method gained attentions in the field of computer experiments in the 80s. Kriging interpolates exactly the experimental design points and provides estimations of the local variance of the predictions, which provides an indication of uncertainty associated with the Kriging model. In the 90s, Kriging had been intensively used in optimisation problems with active learning methods such as efficient global optimisation [83].

The application of the Kriging method in the context of structural reliability is relatively recent, introduced in [84] where Kriging with polynomial regression was compared with finite element interpolation on progressive lattice-samplings with analytical functions. In [85], a Kriging model implemented using the MATLAB toolbox DACE [86] was combined with FORM to compute the structural failure probability, after which the result was further compared with RSM. The sampling strategy to build the Kriging meta-model was improved in [87] by using an active learning approach to iteratively add new samples to the experimental design, which reduces the number of calls to the time-demanding performance function.

Technically, Kriging model is a stochastic interpolation algorithm representing the output of a computer model $\mathbf{M}(\boldsymbol{x})$ as a random process, which is assumed to be a Gaussian random process indexed by $\boldsymbol{x} \in D_{\boldsymbol{X}} \subset \mathbb{R}^M$. The first step of Kriging is to define this stochastic field with its parameters according to a design of experiments. Then, the Best Linear Unbiased Predictor (BLUP) is used to estimate the value in a given point. A Kriging model consists of two parts [88] , as shown in the equation below:

$$\mathbf{M}^K(\boldsymbol{x}) = \boldsymbol{\beta}^T \boldsymbol{f}(\boldsymbol{x}) + \boldsymbol{Z}(\boldsymbol{x}) \tag{23}$$

The first term in the above equation is the linear regression part and the second term is the nonparametric part. The linear regression part is similar to the polynomial model in a RSM, and it consists of the basis functions $\boldsymbol{f}(\boldsymbol{x}) = \{f_1(\boldsymbol{x}), f_2(\boldsymbol{x}), \dots, f_P(\boldsymbol{x})\}^T$ and the regression coefficients $\boldsymbol{\beta} = \{\beta_1, \beta_2, , \dots, \beta_P\}^T$, which needs to be determined. The second part in Eqn. (23) is used to model the deviation from the first term and it consists of the random process $\boldsymbol{Z}(\boldsymbol{x})$, which is assumed to be a Gaussian stationary process with zero mean. The covariance of $\boldsymbol{Z}(\boldsymbol{x})$ can be defined as:

$$Cov\big[Z(x_i), Z\big(x_j\big)\big] = \sigma^2 R\big(x_i, x_j; \boldsymbol{\theta}\big), \quad i, j = 1, \dots, N \tag{24}$$

where N is the number of experimental points, σ^2 the progress variance and $R(x_i, x_j; \boldsymbol{\theta})$ the spatial correlation function, which controls on the smoothness of the model, the influence of other nearby points, and differentiability of the response surface. The correlation function $R = R(x_i, x_j; \boldsymbol{\theta})$ describes the correlation between two samples of the input space, e.g. x_i and x_j, and depends on the hyper-parameter $\boldsymbol{\theta}$. In the context of meta-modelling, it is of interest to provide a prediction Kriging model for a new point $\boldsymbol{x}$. Let $\boldsymbol{\mathcal{X}} = \{\boldsymbol{x}_1, \dots, \boldsymbol{x}_N\}$ denote the set of known points of the computer model whose response is $\boldsymbol{\mathcal{Y}} = \{y_1 = \mathbf{M}(\boldsymbol{x}_1), \dots, y_N = \mathbf{M}(\boldsymbol{x}_N)\}^T$. For a new point $\boldsymbol{x}$, the expected value $\mu_{\hat{Y}}(\boldsymbol{x})$ and variance $\sigma_{\hat{Y}}{}^2(\boldsymbol{x})$ of the Kriging model prediction $\hat{Y}(x)$ can be calculated as [89]:

$$\mu_{\hat{Y}}(\boldsymbol{x}) = \boldsymbol{\beta}^T \boldsymbol{f}(\boldsymbol{x}) + \boldsymbol{r}(\boldsymbol{x})^T \boldsymbol{R}^{-1} (\boldsymbol{\mathcal{Y}} - \boldsymbol{F}\boldsymbol{\beta}) \tag{25}$$

$$\sigma_{\hat{Y}}{}^2(\boldsymbol{x}) = \sigma^2 - [\boldsymbol{f}(\boldsymbol{x})^T \quad \boldsymbol{r}(\boldsymbol{x})^T] \begin{bmatrix} \mathbf{0} & \boldsymbol{F}^T \\ \boldsymbol{F} & \boldsymbol{R} \end{bmatrix}^{-1} \begin{bmatrix} \boldsymbol{f}(\boldsymbol{x}) \\ \boldsymbol{r}(\boldsymbol{x}) \end{bmatrix} \tag{26}$$

where $\boldsymbol{\beta} = (\boldsymbol{F}^T \boldsymbol{R}^{-1} \boldsymbol{F})^{-1} \boldsymbol{F}^T \boldsymbol{R}^{-1} \boldsymbol{\mathcal{Y}}$, $\boldsymbol{F}$ is the information matrix of generation terms, $\boldsymbol{r}(\boldsymbol{x})$ is the correlation vector between an unknown point $\boldsymbol{x}$ and all known experimental points $\boldsymbol{\mathcal{X}}$, and $\boldsymbol{R}$ is the correlation matrix defined by $R_{ij} = R(x_i, x_j; \boldsymbol{\theta}), i, j = 1, \dots, N$.

To construct a Kriging meta-model, the functional basis of Kriging trend $\boldsymbol{f}(\boldsymbol{x})$ needs to be selected properly. Then, an appropriate correlation function $R(x_i, x_j; \boldsymbol{\theta})$ is needed to estimate the unknown parameters $\boldsymbol{\theta}$ by solving the optimization problem. Using the optimal value of $\boldsymbol{\theta}$, the rest of the unknown Kriging parameters $(\sigma^2, \boldsymbol{\beta})$ can be calculated. Finally, predictions for new points can be made in terms of the mean and variance of $\hat{Y}(\boldsymbol{x})$, according to Eqns. (25) and (26). Before providing the Kriging meta-model in Eqn. (23), the unknown hyper-parameters need to be estimated by solving an optimization problem. The Maximum Likelihood Estimation (MLE) and the Cross-Validation (CV) methods are among the most popular approaches to estimate the best parameters of the spatial correlation functions [90].

The Kriging meta-models predict the value of the limit state surface most accurately in the vicinity of the experimental design samples $\boldsymbol{\mathcal{X}}$, but these samples are generally not optimal to estimate failure probability. Thus, an Adaptive Kriging Monte Carlo Simulation (AK-MCS) was introduced in [88, 91] to improve the accuracy of the surrogate model in the neighbourhood of the limit state function. Using an actively learning method, AK-MCS adaptively establishes the Kriging meta-model, which is then combined with MCS to evaluate the probability of failure. By using the Kriging meta-model to approximate the limit state function, AK-MCS save the costly evaluation of the actual limit state function. There have been different learning functions reported in the literature to use with Kriging [87, 88, 92, 93].

3.3.3 The moment method

The moment method [75, 94, 95] computes the statistical moments of the limit state function and fits these moments with an empirical distribution system such as the Johnson system, the Pearson system, and Gram-Charier series etc. The fitted distribution is then used to calculate the probability of failure. Unlike RSM and Kriging methods, which build surrogate models for the limit state function, the moment method builds the surrogate models for the probability distribution of the limit state function. Different methods have been proposed to evaluate the statistical moments required, including the generalised method of moments [96], the high-dimensional model representation [97] and the dimension reduction method [98]. A nonlinear system of equations for point estimate of probability was combined with the Johnson distribution system and Gram–Charlier series in [99]. Five-moment method formulas were investigated in [100], where a point estimate using Rosenblatt transformation and quadrature points for each random variable were adopted. A design of experiment technique was proposed in [101], to use three level experiments for each random variable to calculate the first two moments of the limit state function. This approach was further improved in [102] where levels and weighs were set equivalent to the nodes and weights in the Guass-Herminte quadrature formula. The approach was further extended by [95] from normally distributed random variables to non-normal cases, by deriving an explicit formulation of three levels and weights for general distributions. The fourth-moment method was suggested in [103].

The cost of the moment method can be high, as it increases exponentially with the increase of random variables. Among others, one way to reduce the associated computational cost is the univariate dimension reduction method [98, 104], which decomposes the multi-dimensional performance function into multiple univariate functions, therefore accelerating the calculation of the N-dimension statistical moment integration. Specifically, the performance function $g(\boldsymbol{x})$ is approximated by a sum of univariate functions, depending on only one random variable with the other variables fixed to the reference point.

4 Stochastic finite element methods

Unlike the deterministic FEM, which has a standard Galerkin formulation, the SFEMs do not have a unique and generally agreed framework. Instead, there are various SFEM approaches, such as the perturbation method, the polynomial chaos expansion method, the stochastic collocation method, joint diagonalization method etc. [105]. These different SFEM approaches all have their own advantages and drawbacks, and they have been formulated following various assumptions and have different mathematical setups. At the highest level, SFEM schemes can be roughly classified into two groups: intrusive methods and non-intrusive methods. The intrusive methods rely on dedicated formulations of a stochastic version of the original model. As such, their solution schemes have to be derived from scratch for each new class of problems. The non-intrusive methods, however, do not require modification to the deterministic FEM codes, which is a major advantage for analysing reliability problems involving complex FE analysis. These methods typically build surrogate models to approximate the system response based on sample solutions. It is worth to note that the SFEM is still in its early stage and further development is needed to advance the SFEM to a level where both reasonable mathematical accuracy and sufficient computational efficiency are achieved. All major SFEM approaches are briefly recapped in the following subsections, while their technical details are referred to the original papers or the summary papers where appropriate.

4.1 The perturbation method

The perturbation stochastic finite element method can estimate the mean and covariance of the system response [106-108], with very wide applications in different engineering fields, including geotechnical problems [109, 110], nonlinear dynamic problems [111], to name a few. The main idea of the perturbation method is to expand all input random variables with respect to their respective mean values via Taylor expansion, which can then be used to derive the analytical expression for the variation of desired system response due to a small variation of those random variables. The unknown coefficients in the expansion are obtained by grouping like polynomials and cancelling the corresponding coefficients. The main limitation of the perturbation method is on its accuracy, which holds only for low-level input uncertainties [112, 113]. The standard perturbation scheme does not provide higher-order statistical estimates, and there is no easy way to extend the formulation to the higher-order situation without invoking significantly complicated implementation and greatly increased computational cost.

4.2 The Neumann expansion method

Proposed in [114, 115], the Neumann expansion method uses a truncated series expansion to approximate the solution of a discretized linear equation system, avoiding the cost of a direct matrix inversion. The method was further applied to non-linear static and dynamic problems [116], and also to cover geometric uncertainties [117]. The first step of the Neumann expansion method is to split the stochastic stiffness matrix and load vector into their corresponding mean and random deviatoric parts. Then expanding the stiffness matrix by Neumann expansion yields:

$$\boldsymbol{u} = \sum_{r=0}^{\alpha}(-\boldsymbol{Q})^r \boldsymbol{u}_0 + \sum_{r=0}^{\alpha}(-\boldsymbol{Q})^r {\boldsymbol{K}_0}^{-1} \Delta \boldsymbol{F} \tag{27}$$

The above Neumann expansion converges if all eigenvalues of $\boldsymbol{Q} = {\boldsymbol{K}_0}^{-1}\Delta \boldsymbol{K}$ are always less than unity [118]. The computational cost of the Neumann expansion method increases with the number of terms required in Eqn. (27). Therefore, for problems with large random fluctuations, the Neumann expansion series may lose its advantage, and it could become even more expensive than the direct Monte Carlo method [118]. To overcome this computational difficulty and enhance the computational efficiency of matrix inversions, improvements

have been made by combining the Neumann expansion method and the preconditioned conjugate gradient method [119]. Another way to improve the efficiency and the accuracy is by introducing the convergence parameter λ, which can be determined as a solution to a distance minimization problem for an approximation of the inverse of the system matrix [120].

4.3 Joint diagonalization strategy

As a general strategy to solve stochastic linear systems, the Joint Diagonalization (JD) method [105, 121, 122] is applicable to any real symmetric matrices. The main idea of JD is to simultaneously diagonalize all matrices in the system to obtain an average eigen-structure using a sequence of orthogonal similarity transformation, which gradually decreases the off-diagonal elements of the matrices. The stochastic linear algebraic system is then decoupled by joint diagonalization, and its approximate solution is explicitly obtained by inverting the resulting diagonal stochastic matrix and performing the corresponding similarity transformation. For joint diagonalization, the classical Jacobi method is modified to solve the resulting average eigenvalue problem. The strategy is simply an approximation except if all the matrices have exactly the same eigen-structure. In this approach, the linear static equation $\mathbf{Ku} = \mathbf{F}$ is first reorganized as follows:

$$(\boldsymbol{K}_0 + \xi_1 \boldsymbol{K}_1 + \xi_2 \boldsymbol{K}_2 + \cdots + +\xi_m \boldsymbol{K}_m)\boldsymbol{u} = \boldsymbol{F} \tag{28}$$

where $\boldsymbol{K}_j, \forall$ are real symmetric deterministic matrices and $\xi_j, \forall$ are random variables. Assuming that there existing an invertible $\boldsymbol{Q}$ to simultaneously diagonalize all matrices $\boldsymbol{K}_j, \forall$ such that:

$$\boldsymbol{Q}^{-1}\boldsymbol{K}_j\boldsymbol{Q} = \boldsymbol{\Lambda}_j = diag(\lambda_{j1}, \lambda_{j2}, \dots, \lambda_{jn}), \quad (j = 1, \dots, m) \tag{29}$$

where $\lambda_{ji}, (i = 1, \dots, n)$ are eigenvalues of the $n \times n$ real symmetric matrix $\boldsymbol{K}_j, \forall$. The product of the Givens rotation matrices forms the transform matrix

$$\boldsymbol{Q} = \boldsymbol{G}_1^T \boldsymbol{G}_2^T \dots \boldsymbol{G}_k^T, \tag{30}$$

where $\boldsymbol{G}_j = \boldsymbol{G}_j(p, q, \theta)$ is the Givens rotation matrices and k is the total number of Givens transformations. After determine the transformation matrix and eigenvalues the random equation system can be readily calculated.

$$\mathbf{u} \approx \mathbf{Q}(\boldsymbol{\Lambda}_0 + \xi_1 \boldsymbol{\Lambda}_1 + \cdots + \xi_m \boldsymbol{\Lambda}_m)^{-1} \boldsymbol{Q}^{-1} \boldsymbol{F} \tag{31}$$

The major computational cost of the proposed approach is the Jacobi-like joint diagonalization procedure which is proportional to the total number of matrices m. This implies that the algorithm can be easily parallelized and the total computational cost is proportional to the total number of random variables in the system.

4.4 Polynomial chaos expansion

Introduced by Ghanem and Spanos [5], the Polynomial Chaos Expansion (PCE) approach uses Hermit polynomials of Gaussian random variables (known as polynomial chaos expansion or Wiener chaos expansion) to represent the solution of the stochastic equations. By using a Galerkin scheme to project the random solution onto the Hermit polynomials, the solution can be resolved in the form of PCE coefficients by solving a deterministic equation system. The classical PCE based on Hermit polynomials have been extended to the so-called generalised polynomial chaos expansion (gPC), by using different orthogonal polynomial basis functions corresponding to the probability distributions of other non-normal variables [123-125]. The PCE approach provides a very flexible framework to investigate numerical solutions for stochastic partial differential equations, and practically it has marked the foundation of SFEM as an independent and fast growing research field in computational mechanics and computational engineering. The PCE scheme has been researched in a very wide context of engineering problems, ranging from structural dynamics and random vibrations to computational fluid dynamics and thermodynamics problems [126-128]. The basic theory of PCE is outlined below, while the various PCE-based SFEM approaches are summarized in the following subsections. For simplicity, all SFEM techniques that directly or indirectly related to PCE are grouped together in this section. It is noted that for different emphasis, the methods reviewed here may well be considered as independent techniques in other literatures.

In the PCE approach, any second-order random variable or stochastic process, i.e. the quantities with finite variance, may be expanded as follows:

$$\boldsymbol{Y} = \sum_{\alpha \in \mathbb{N}^M} y_\alpha \psi_\alpha(\boldsymbol{\xi}) \tag{32}$$

where $\psi_\alpha(\boldsymbol{\xi})$ are a set of basis functions, y_α refer to the deterministic coefficients to be solved, $\boldsymbol{\xi}$ represent standard normal random variables vector, $\boldsymbol{\alpha} = \{\alpha_1, \dots, \alpha_M\}$ is the multi-index, and M is the number of input random variables. These basis functions form the approximation space and can be represented by some orthogonal polynomials. For $M-$ dimensional of PCE up to order p, the total number of terms P required in the expansion is:

$$P = \binom{M+p}{p} = \frac{(M+p)!}{M!p!} \tag{33}$$

The number of polynomials P in the expansion grows very fast for small increases in p, or in the number of the random variables M [129].

The PCE method can be classified into intrusive and non-intrusive approaches. The Galerkin method is the best example for intrusive approach [130-132]. The non-intrusive approaches include the probabilistic collocation method [133] and the sparse quadrature [134], which depend on repeated running of the computational model for selected realisations of random variables $\boldsymbol{X}$.

4.4.1 The Galerkin solution schemes

In this approach, the PCE coefficients are determined by solving a system of linear equations derived by making the residual to be orthogonal to the approximation space. Considering the linear static elastic analysis equation $\boldsymbol{Ku} = \boldsymbol{F}$ with n degree of freedom, the Galerkin based PCE formulation leads to a linear system of size $(n.P \times n.P)$, which reflects the high computational cost associated with the standard PCE approach. A number of improvements have been reported to increase the computational efficiency while keeping the memory usage to a minimum [135-137]. As the block diagonal of the system are fully determined by a single component matrix $\boldsymbol{K}_0$, whereas $\boldsymbol{K}_i$ represent the random fluctuations and have the same sparsity structure, the block Gauss-Jacobi preconditioning was proposed for cost reduction [138]. An iterative solution was suggested in [139] to avoid the assembly of the $(n.P \times n.P)$ matrix system and solve the systems $[\boldsymbol{k}_{jk}]\{\boldsymbol{u}_k\} = \{\boldsymbol{F}_j\}$ which requires only the storage of the deterministic size $\boldsymbol{K}_i$ matrices and the corresponding $\langle \xi_i \psi_j \psi_k \rangle$ coefficients. The preconditioned conjugate gradient solvers have also been adapted to the solution of linear SFEM system [140, 141].

The accuracy of the Galerkin based PCE was checked in terms of representing the probability density function of the strain values for the composite panel structure [142]. It was found that low-order (such as 1-2) PCE provided reasonable accuracy, but higher-order expansion was required to achieve good accuracy in the tails of the distribution, which are essential in reliability analysis. Furthermore, it is noted that the results become unstable and highly inaccurate, where the stiffness has been modelled using normally distributed random parameters and the variation of these parameters exceed 30%. This is because the assumption of Gaussian random fields allows zero or negative values for the stiffness matrix, which is non-physical.

4.4.2 Collocation method

Stochastic collocation method estimates the PCE coefficients by calculating the stochastic response at selected points in the multidimensional space of the input random variables, which are referred to as the collocation points. Due to the orthogonality of the PCE basis, the deterministic coefficients (y_i) for the PCE approximation of a random parameter ($\boldsymbol{Y}$) are estimated as

$$y_i = \frac{1}{\langle \psi_i^2 \rangle} \int \boldsymbol{Y}.\psi_i.f(\boldsymbol{\xi}).d\boldsymbol{\xi} \tag{34}$$

where $f(\boldsymbol{\xi})$ represents the joint PDF of the random vector $\boldsymbol{\xi}$. Thus each coefficient y_i is nothing but the orthogonal projection of the random response $\boldsymbol{Y}$ onto the corresponding basis function ψ_i.

The primary computational effort arises from the evaluation of the above integral, which is performed usually by either deterministic techniques, i.e. the tensor product method [143, 144] and sparse grid method

[145-147], or probabilistic approaches, i.e. Monte Carlo simulation. Recently quasi-random numbers [148] have also been investigated as an alternative option to replace Monte Carlo [149] simulation. The simplest general technique for approximating the multidimensional integral is to employ a tensor product of one-dimensional quadrature rules. In this case, a so-called product grid is constructed, where the total number of points is the product of the number of integration points in each dimension. However, the tensor products would require an unacceptably high number of function evaluations for high dimensional integrals. To address this deficiency, Smolyak's quadrature [145] is often employed, which reduces dramatically the number of collocation points, while conserving a high level of accuracy. It makes use of sparse and nested grids, where the function evaluations are performed only at important points, and furthermore the points used at one level can be re-used in the next one.

Instead of directly estimating the PCE coefficients from Eqn. (34), the least-square regression was adopted in [132] to fit the PCE model on a set of specially selected collocation points. A critical aspect of the linear regression approach is the choice of data points, for which the LHS has been commonly adopted. Moreover, quasi-random sequences such as the Sobol' or Halton sequence have also been adopted in the experimental design [150]. The reference [151] selected the points corresponding to the roots of the orthogonal polynomial of one degree higher than the maximum order of the current PCE. However, different selections of experimental design points can result in different coefficients, which raise questions to the stability of the regression techniques. Furthermore, it was shown in [152] that the selection number of $2P$ [151] does not yield accurate estimations in most applications, and sequentially an empirical rule of $(M-1)P$ regression points was suggested. The minimal size of the experimental design points required for an accurate solution of the regression problem [153] may even make the computation intractable in high dimensions.

It is desirable to predict in advance the truncation error, to guide the selection of the maximal polynomial degree of PCE. The standard procedure is to test several truncation schemes of increasing polynomial degrees and check the convergence for the interest quantities. A posteriori error estimate was suggested in [154] to evaluate the accuracy of any truncated PCE. In order to obtain a fair error estimation within reasonable computational cost, the leave-one-out (LOO) cross-validation [155] can be adopted. The main idea of LOO is to build the surrogate model and compute the error by using different sets of experimental design points.

The main drawbacks of the PCE based SFEM approaches is the high computational costs. Even a low-order PCE can lead to a large number of unknown coefficients, and therefore the experimental design may become unaffordable. Most PCE terms correspond to polynomials representing interactions between input variables, but in many practical applications the high order interactions terms are insignificant and even negligible. Some sparse representations of the truncation have been studied in [154, 156-158] to reduce the computational cost, where the least-angle regression (LARS) algorithm was proposed to keep only the most influential polynomials.

4.4.3 Combining PCE and Kriging (PCK)

The PCE approximation may become inefficient for high nonlinear performance function with a large number of random variables [159, 160]. To overcome this problem, the PCE with LARS and the universal Kriging model were combined to obtain a new family of the optimized meta-model [161]. The PCE treats the global behaviour of the model whereas Kriging interpolates the local variations as a function of the nearby experimental design points. The new technique is defined as a universal Kriging model:

$$\mathbf{M}^{PCK}(\boldsymbol{x}) = \sum_{\alpha \in \mathbb{N}^M} y_\alpha \psi_\alpha(\boldsymbol{\xi}) + \boldsymbol{Z}(\boldsymbol{x}) \tag{35}$$

where the first term is an orthogonal PCE describing the trend of the model, whereas the second term is used to model the deviation from the main trend, and it consists of a Gaussian stationary process with zero mean and the covariance as introduced in Eqn. (24). The purpose of this technique is to choose polynomials that bring the most relevant information to the Kriging meta-model. Note that the new surrogate model can be interpreted as a universal Kriging model, the trend of which consists of a set of orthogonal polynomials. There are two ways to combine the PCE and Kriging: sequential PC-Kriging and optimal PC-Kriging.

In Sequential PC-Kriging (SPCK), the set of polynomials and the Kriging meta-models are determined sequentially. Firstly, the optimal set of the polynomials is determined by the LARS algorithm. Then these results can be used as a suitable trend for the universal Kriging model. At the end of the algorithm, the accuracy of the calibrated meta-model can be estimated by determine the LOO error. In the Optimal PC-Kriging (OPCK), the PC-Kriging meta-model is obtained iteratively. As in SPCK, the optimal set of polynomials is evaluated by LARS. The LARS algorithm results in a sparse set of polynomials which are ranked according to their correlation to the current residual at each LARS iterations (in decreasing order). Each polynomial is then added individually to the trend of a PC-Kriging model. In each iteration, a new PC-Kriging model is calibrated.

5 Comparative studies

In this section, four examples are tested to compare the performance of the representative SRA and SFEM approaches reviewed above and to extract general guidelines for selecting the most appropriate UQ approach for specific application needs. The first example consists of a group of explicitly defined limit functions under different nonlinearities and different number and type of random inputs. The rest examples are based on different structural problems with the presence of both continuous and discontinuous uncertainties.

5.1 Examples for explicit limit-state functions

As listed in Table 1, several commonly used limit state functions are tested in this example. The reference values are obtained using the crude Monte Carlo simulation. The failure probability together with the time and the number of functional calls are evaluated for each case. The results for cases 1, 2, 3 and 4 are shown in Tables 2, 3, 4 and 5 respectively. These cases are investigated to demonstrate the accuracy, efficiency and robustness of different reliability methods.

Case 1 is a linear limit-state function with noise terms, where the FORM gives acceptable results for the reliability index but the SORM gives very poor results. This is because the noise terms in the performance function causes the total principal curvatures of the limit state surface exceeding the applicable range of SORM. If the noise term is removed from the performance function, the probability of failure will convergent to the exact solution ($P_f^{SORM} = 1.264 \times 10^{-2}$). The limit state function in **u** space and FORM iteration for case 2 are shown in Figures 1a and 1b. In this case, FORM has significant errors for the performance function with multiple MPP problems, as shown in Table 3. This means that FORM is not suitable for performance function with multiple MPP. The same reason explains the bad result by SORM. The results given in Table 4 shows that FORM and SORM both provide quite good results for slightly non-linear problem as given in case 3 compared with those of MCS, i.e. with a relative error equal to 5.99% and 0 for FORM and SORM, respectively. However, this is not the case for concave limit state function given in case 4 where FORM and SORM both fail to converge.

The IS has been proposed to reduce the number of samples in the conventional MCS. This technique can shorten the computational time to a certain extent as shown in all results except for the case 4 (concave limit state function). The SS approach is applied with a conditional failure probability at each level equal to $p_0 = 0.1$ and with the number of samples set to $N = 500$ at each conditional level. The number of conditional levels is chosen to cover the required response level whose failure probability is estimated. From Tables 2, 3, 4 and 5, it is seen that the average values of failure probability produced by SS/MCMC mostly agree with the results of MCS. Figure 1c plots the number of subsets for case 2; however, it uses seven subsets until the results converge. The value obtained for the probability of failure with the combined DS and IS method, gives good accuracy with less than 1% relative error.

The RSM approach can provide results with sufficient accuracy for certain cases, but becomes computationally impractical for problems including a large number of nonlinear random variables or with multiple MPPs. Besides, it is hard to build the appropriate response surface without knowing the location of MPP, and there is no guarantee that the surrogate surface is a sufficiently close fit in all regions of interest.

The random variables in case 1 are independent lognormal variables. Let $\{Z_i\}_{i=1}^6$ be Gaussian random variables $\mathrm{N}(0,1)$. By employing Hermite polynomials to approximate $\{X_i\}_{i=1}^6$ we get:

$$X_i \approx X_{N.i}(Z_i) = \sum_{k=0}^{N} c_{i,k} H_k(Z_i), \quad c_{i,k} = \exp(\mu_i + \frac{\sigma_i^2}{2}) \frac{\sigma_i^k}{k!} \tag{36}$$

Then the surrogate model can be constructed as follows:

$$g_N(Z) = X_{N.1} + 2X_{N.2} + 2X_{N.3} + X_{N.4} - 5X_{N.5} - 5X_{N.6} + 0.001\sum_{i=1}^{6}\sin(100X_{N.i}) \quad (37)$$

Adaptive LARS is now compared to OLS algorithm with the degree of polynomial $p = 2$. From the results of case 1, it can be observed that adaptive LARS appears to be more efficient than OLS. In particular, it yields a relative error $err_{LOO} = 5 \times 10^{-4}$ using only $N = 40$ model evaluations, whereas $N = 120$ simulations are used for OLS algorithm to get $err_{LOO} = 0.0023$. However, with a sufficient number of samples of performance function, an accurate failure probability estimation can always be obtained.

The Kriging meta-model based MCS procedure is also applied to these cases. First, an initial Kriging predictor is built for the limit-state function using 100 uniformly generated points within a hypersphere. Based on this initial prediction, the refinement procedure introduced in AK-MCS is then used to add new points at each refinement iteration. As can be seen from Table 2~Table 5, the results provided by Kriging meta-model method are quite close to those given by MCS, which means that the Kriging predictor is rather accurate in all cases.

The full factorial moment method (FFMM) give accurate results for cases 1,2,3 and 4 but with high computational cost for cases 1 and 3. This is due to the exponential increase of computation time with input dimension. Thus, it is only suitable for low-dimension.

Table 1 Limit-state functions description

Case	Limit-state functions	Random variables	Description	Ref.
1	$g = x_1 + 2x_2 + 2x_3 + x_4 - 5x_5 - 5x_6 + 0.001\sum_{i=1}^{6}\sin(100x_i)$	$x_{1-4}: LN(120,12)$ $x_5: LN(50,15)$ $x_6: LN(40,12)$	Linear limit state function with noise term	[31]
2	$g = x_1x_2 - 146.14$	$x_1: N(78064.4,11709.7)$ $x_2: N(0.0104,0.00156)$	Multiple MPPs	[31]
3	$g = 2 + 0.015\sum_{i=1}^{9}x_i^2 - x_{10}$	$x_{1-10}: N(0,1)$	Quadratic limit state function with 10 terms	[162]
4	$g = -0.5(x_1 - x_2)^2 - \frac{(x_1 + x_2)}{\sqrt{2}} + 3$	$x_{1-2}: N(0,1)$	Concave limit state function	[163]

Table 2 Comparison of reliability approximations for case 1: $cov_{P_f} = 0.01$

Method	$P_f \times 10^{-2}$	β	Function calls	Time (sec)	Relative error ε_β %
FORM	0.943	2.3481	1165	1	4.2
SORM (Curvature Fitting method)	0.00055	4.3950	1245	1.02	95
SORM (Curvature Fitting method)	0.00076	4.3255	1245	1.02	95
MCS	1.212	2.2533	820000	1.5	Reference
IS	1.200	2.2572	6565	1.2	0.17
DS+IS	1.190	2.2511	2680	0.75	0.1
Subset Simulation	1.220	2.2511	18994	0.11	0.1
RSM (second order without cross term) +IS	1.240	2.2455	650	3.45	0.35
PCE – Quadrature (Smolyak)	1.160	2.2708	455	0.49	0.78
PCE – OLS	1.182	2.2629	120	0.34	0.42
PCE – LARS	1.227	2.2485	40	0.25	0.21

AK-MCS	1.213	2.2530	40	35	0.01
Moment method-Zhao & Ono	1.219	2.2511	42	0.07	0.098
Moment method-FFMM	1.212	2.2533	729	1.2	0

Table 3 Comparison of reliability approximations for case 2: (multiple MPPs) $cov_{P_f} = 0.1$

Method	$P_f \times 10^{-7}$	β	Function calls	Time (sec)	Relative error ε_β %
FORM	0.285	5.428	20	0.03	5.83
SORM	Found curvatures >= 1				
MCS	1.460	5.1285	$> 10^9$		
IS	1.1791	5.1686	8220	0.2	0.78
DS+IS	1.610	5.1101	57		0.34
Subset Simulation	1.418	5.134	57134	0.72	0.11
RSM (second order without cross term) +IS	Not converged				
Non-intrusive PCE – Quadrature (Smolyak)	1.604	5.110	30	0.7	0.36
Non-intrusive PCE – OLS (Full PC)	0.803	5.240	80	0.13	2.17
Non-intrusive PCE – LARS (Sparse PC)	1.5054	5.1220	75	80	0.12
AK-MCS	1.501	5.1233	30	30	0.10
Moment method-FFMM	1.3255	5.1467	9	0.04	0.35

Table 4 Comparison of reliability approximations for case 3: (quadratic LS 10 terms).

Method	$P_f \times 10^{-2}$	β	Function calls	Time (sec)	Relative error ε_β %
FORM	2.28	2.00	24	0.02	5.97
SORM	1.67	2.127	236	0.03	0
SORM (Breitung)	1.75	2.108	236	0.03	0.89
MCS	1.67	2.127	590000	1.07	Reference
IS	1.62	2.138	27124	0.96	0.52
Subset Simulation	1.65	2.131	18999	0.1	0.19
RSM (second order without cross term) +IS	1.64	2.135	1050	2.9	0.38
PCE – Quadrature (Smolyak)	1.75	2.108	1771	2.45	0.89
PCE – OLS	1.71	2.117	500	0.33	0.47
PCE – LARS	1.68	2.126	250	0.27	0.05
AK-MCS	1.53	2.1628	40	40	1.68
Moment method-FFMM	1.4871	2.1735	59049	0.04	2.19

Table 5 Comparison of reliability approximations for case 4: (concave LS).

Method	$P_f \times 10^{-1}$	β	Function calls	Time (sec)	Relative error ε_β %
FORM			No convergence		
SORM			No convergence		
MCS	1.0537	1.2516	90000	0.137	-
IS	1.0411	1.2584	2,191,012	190	0.54
DS+IS	1.02	1.2702	32	75	1.49
Subset Simulation	1.0680	1.2437	10000	0.1	0.63
RSM (second order without cross term) +IS			No convergence		
PCE – Quadrature (Smolyak)	0.994	1.2849	30012	0.6	2.7
PCE – OLS	1.0469	1.2553	20	0.20	0.29
PCE – LARS	1.0408	1.2586	15	0.17	0.55
AK-MCS	1.0458	1.2559	28	3.5	0.34
Moment method-FFMM	1.137	1.2071	9	0.04	3.56

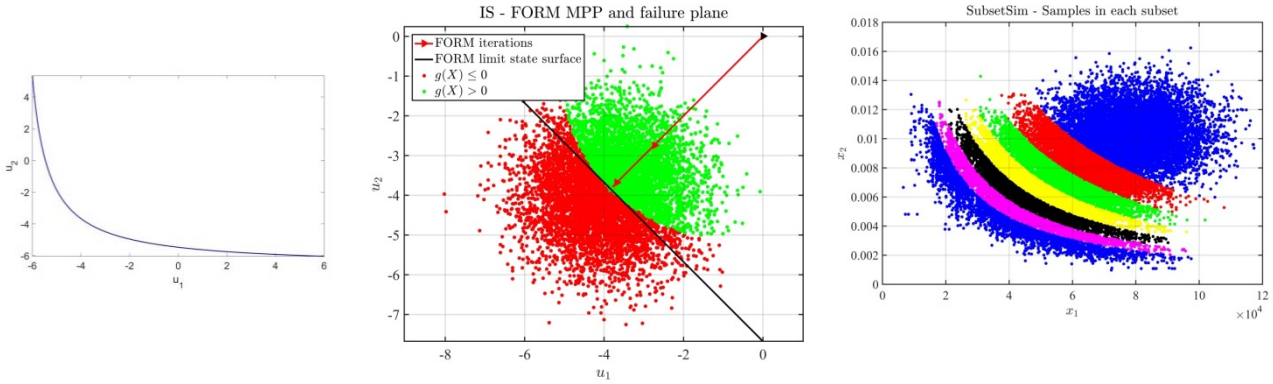

(a) (b) (c)

Figure 1. Case 2 multiple MPPs. (a) Limit state function in U space. (b) FORM iteration and limit state function. (c) Graphical visualization of the convergence of the subset simulation analysis.

5.2 Tunnel analysis

A plane strain problem of a simplified tunnel model is considered in this example, and the geometry and load parameters are shown in Figure 2a. The deterministic parameters which considered in this example are the unite weight of the rock mass $\gamma = 25\,kN/m^2$, Poison's ratio $\nu = 0.3$ and the surcharge load $p = 1900\,kPa$. While Young's modulus of elasticity of the rock is considered spatially varying with $mean(E(\boldsymbol{x},\omega)) = 15 \times 10^8$ Pa and $Cov(E(\boldsymbol{x}_1,\omega), E(\boldsymbol{x}_2,\omega)) = 5.0625 \times 10^{16} \exp(-\frac{(x_2-x_1)^2+(y_2-y_1)^2}{4})$ Pa^2. A plane-strain finite element mesh consisting of 267 nodes and 472 triangular elements is shown in Figure 2b. Subject to surcharge load, the maximum settlement of the tunnel is taken as the key factor for measuring the serviceability of the tunnel, thus the performance function is expressed as:

$$g\big(E(\boldsymbol{x},\omega)\big) = \delta_{max} - |u(E(\boldsymbol{x},\omega))| \tag{38}$$

where δ_{max} is the maximum allowable settlement at the top of the tunnel, and $u(E(\boldsymbol{x},\omega))$ is the crown settlement dependent on the random field $E(\boldsymbol{x},\omega)$. For illustrative purposes, the maximum allowable settlement is assumed to be 20 mm. As no exact K-L expansion solution is available for representing this random field, only the F-K-L discretisation is used for this stochastic field. In order to determine the number of random variables needed in the F-K-L discretization, the approximation error due to truncation is controlled within 10% in terms of the difference of variance, which leads to 13 random variables. A specific realization of the random Young's modulus field of the rock is shown in Figure 2c, where the random Young's modulus varies significantly by -30% and 20% from the mean value. The stochastic system of linear algebraic equations

is composed of fourteen 534×534 real symmetric matrices including the mean matrix. The failure of probability, reliability index, number of evaluation model and computational time are investigated using different SRA and SFEM methods, and the results are summarized in Table 6.

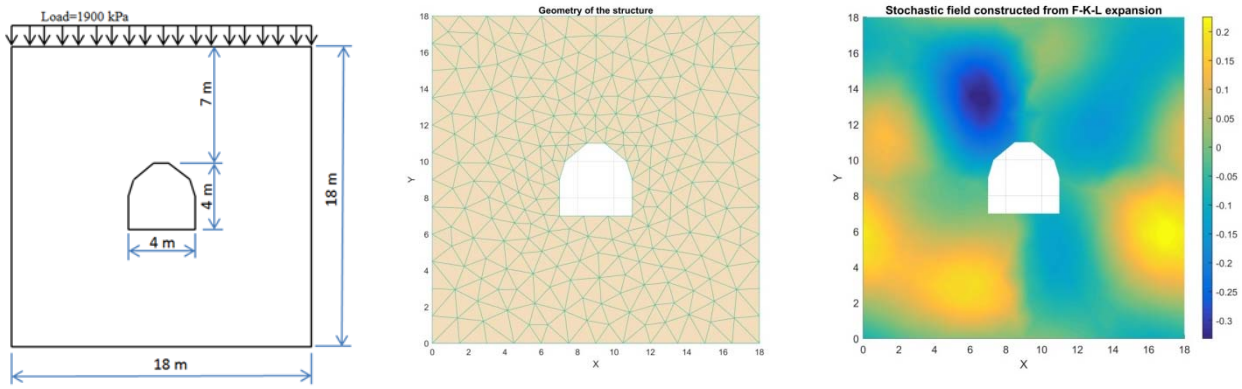

(a) (b) (c)

Figure 2. (a) Geometry of the underground tunnel. (b) Finite element mesh and boundary conditions of the tunnel. (c) Young's modulus of elasticity for the rock reconstructed from F-K-L expansion.

The reference result is obtained as 2.6345 for the reliability index and 4.2130×10^{-3} for the probability of failure from MCS with 1,000,000 simulations, where $COV = 1.5\%$ as shown in Figure 3b. From Table 6 and Figure 3a, the following observations are made:

- The FORM is inaccurate in dealing with such large number of random variables with a nonlinear performance function.
- SORM and RSM have similar results and are reasonably accurate compared with the MCS reference with relative errors of 0.67% and 0.83% in reliability index respectively. According to the number of model evaluations, RSM is more efficient than SORM in this test.
- The JD method obtains a good path-wise solution (strong solution) to the probability of failure with the best accuracy and low computational cost with the ratio of the off-diagonal entries to the Frobenius norm is 6.024×10^{-3}. Nevertheless, when the magnitude of the uncertainties becomes large (more than 20%), the JD scheme yields an oscillating solution, which gives poor results see Figure 5a and Figure 5b. Moreover, for problems with the probability of failure in an order higher than 10^{-3}, the JD leads to less accurate results compared with other reliability methods, see Figure 4a and Figure 4b.
- The instructive PCE (based on a 3rd order expansion, 13 random variables, and total degree of freedom at 534) requires to solve a large system of 299040 linear equations in order to determine the PCE coefficients. To reduce the cost, the non-intrusive methods OLS and LARS are tested in this example, where the adaptive LARS procedure converges at the cost of only N = 700 runs and gives an accurate result for the probability of failure. The obtained PCE provides a normalized LOO error of 8.8977e-04.
- The results obtained from the AK-MCS compare very well to the reference as soon as N = 140 points are used in the experimental design, see Figure 3c. The error is less than 0.2% in the generalized reliability index for probabilities of failure in the order of 10^{-3}.

Table 6 reveals that in relative terms, the JD, AK-MCS and PCE-LARS schemes have the best balance of accuracy and efficiency. The classical Neumann method converges much slower than all other methods. The intrusive PCE is not particularly suitable for complex structures with many uncertain variables (e.g. 10).

A parametric study is carried out by varying the threshold u from 18 mm to 22 mm to examine the SRA and SFEM methods at different levels of the failure probability and the reliability index. The results are summarized in Table 9, Figure 4a and Figure 4b. The error of the JD method increases with the growth of the failure probability, while the error of other methods increases as the failure probability decreases.

The PDF and CDF of the performance function considered and the number of the experimental design points selected in various SRA methods are plotted in Figures 6a and 6b. Figure 6a shows that the PDF curve obtained from JD differs significantly from the other PDF curves. The PDF curves for other methods are similar and agree well with the MCS result with a sample size of 5000. The CDF curve obtained from the JD is also different from the reference curve except in their tails. This observation confirms that JD is only suitable for evaluating lower-level of failure probability, see Figure 6b. In any case, the accuracy in representing the tails of the CDF of the performance function should be carefully evaluated, as they are the single most critical part for failure probability evaluation.

Figures 5a and 5b show the effect of the coefficient of variance of the input random field cov_E on the probability of failure and the reliability index of the tunnel respectively. It is noted that cov_E has a significant influence on P_f . The increase of cov_E will cause an increase in P_f in this example.

The mean, standard deviation, skewness and kurtosis of the distribution of the crown settlement are also considered. The MCS provides the reference value with a two-digit accuracy (100,000 model evaluations are performed), and the reference mean, standard deviation, skewness and kurtosis are 17.79 mm, 0.75 mm, -0.3221 and 3.1476, respectively. The statistical moments are also estimated using different SRA and SFEM schemes and the results are compared in Table 7. Good accurate estimates of the fourth order moments are obtained by these methods. Also, the results of the fourth statistical moments of the performance function are calculated by various methods and recoded in Table 8. Good results are obtained by these methods except RSM.

Figures 7a and 7b show the effect of (cov_E) on the statistical moments. It is found that the mean and the standard deviation of the settlement are very sensitive to cov_E. For example, when cov_E increases from 0.15 to 0.4, the mean value increases from 17.79 mm to 18.63 mm and the standard deviation increases from 0.54 to 2.6 mm. Also, it is observed that when increasing cov_E, the perturbation and JD methods give poor results for the statistical moments.

Table 6 Comparison of SRA and SFEM methods for the tunnel example.

Method	$P_f \times 10^{-3}$	β	Function calls	Time (sec)	Notes	Relative error ε_β %
FORM	1.9827	2.8809	236	15	-	9.35
SORM (Curvature Fitting method)	4.8704	2.5849	589	30	-	1.88
SORM (Curvature Fitting method)	4.4370	2.6169	589	30	Improved Breitung	0.67
MCS	4.2130	2.6345	1,000,000	40766	$cov_{P_f} = 0.015$	
IS	4.2270	2.6334	45736	1666	$cov_{P_f} = 0.01$	0.04
Subset Simulation	4.590	2.6053	2800	115	$cov_{P_f} = 0.197$	1.11
RSM (second order without cross term) +IS	4.4921	2.6127	116	14	$cov_{P_f} = 0.01$	0.83
Neumann Expansion	4.2270	2.6334	45736	2134	$cov_{P_f} = 0.01$	0.04
MCS with Neumann-Lambda-first	4.0213	2.6503	37141	1692	$cov_{P_f} = 0.01$	0.60
Intrusive PCE (Galerkin)	-	-	-	-	-	-
Non-intrusive PCE – Quadrature (Smolyak)	4.4905	2.6128	3654	255	Error= 6.766e-4	0.82
Non-intrusive PCE – OLS (Full PC)	4.6108	2.6037	700	45	LOO = 4.924e-05 $p = 3$ Size of full basis: 118	1.17
Non-intrusive PCE – LARS (Sparse PC)	4.1797	2.6372	350	33	LOO 8.8977e-04 $p = 3$ Size of sparse basis: 115	0.1
AK-MCS	4.2850	2.6287	140	427	$cov_{P_f} = 0.015$	0.22

Joint diagonalization + IS	4.2181	2.6341	---	323	0.02

Table 7 Comparison of moment analysis for the crown settlement of the tunnel

Method	μ_U cm	σ_U cm	Function calls
MCS	17.79	0.75	100,000
RSM (second order without cross term)	17.78	0.721	116
Intrusive PC -Galerkin	-	-	-
Non-intrusive PCE – OLS (Full PC)	17.79	0.75	1000
Non-intrusive PCE – LARS (Sparse PC)	17.79	0.75	700
Perturbation (Second order)	17.68	0.76	-
MCS-Neumann	17.79	0.75	50
Kriging	17.66	0.75	80
Joint diagonalization	17.61	0.76	50

Table 8 Comparison of statistical moment for performance function $g\big(E(\boldsymbol{x},\omega)\big) = \delta_{max} - |u(E(\boldsymbol{x},\omega))|$.

Statistical moments	MCS	Joint diagonalization	Neumann	RSM	Kriging	PCE-OLS	PCE-LARS
Mean mm	2.21	2.39	2.21	2.22	2.21	2.21	2.21
Standard deviation mm	0.751	0.818	0.751	0.722	0.751	0.7591	0.751
Skewness	-0.3221	-0.3074	-0.3221	-0.1693	-0.3221	-0.3213	-0.3062
Kurtosis	3.1476	3.1305	3.1476	2.9464	3.1476	3.1411	3.0787

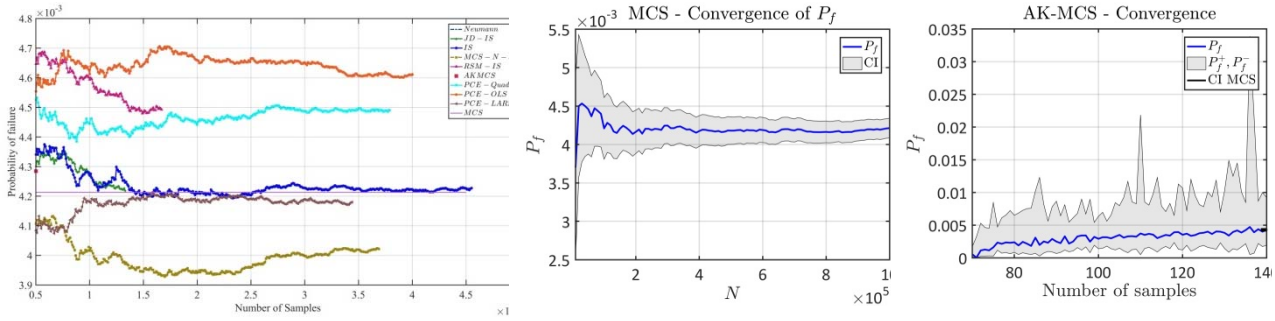

(a) (b) (c)

Figure 3. (a) The convergence of the probability of failure for different reliability methods, (b) Monte Carlo convergences, and (c) AK-MCS convergence.

Table 9 Estimates of the generalized reliability index for various values of the threshold settlement of the tunnel

Threshold mm	Reference IS	FORM		SORM		Subset		RSM	
	Beta	Beta	error	Beta	error	Beta	error	Beta	error
18	0.317	0.561	76.9%	0.444	40.0%	0.332	4.7%	0.296	6.5%
19	1.528	1.793	17.3%	1.571	2.8%	1.501	1.8%	1.537	0.6%
20	2.633	2.881	9.4%	2.617	0.6%	2.605	1.1%	2.613	0.8%
21	3.539	3.842	8.6%	3.550	0.3%	3.602	1.8%	3.553	0.4%
22	4.370	4.686	7.2%	4.373	0.1%	4.452	1.9%	4.394	0.6%

Cont. Table 9 Estimates of the generalized reliability index for various values of the threshold settlement of the tunnel

Threshold mm	PCE-OLS		PCE-LARS		AKMCS		JD		Neumann	
	Beta	error	Beta	error	Beta	error	Beta	error	Beta	error
18	0.339	7.0%	0.322	1.7%	0.306	3.5%	0.502	58.4%	0.328	3.5%
19	1.546	1.2%	1.526	0.1%	1.516	0.8%	1.632	6.8%	1.553	1.7%
20	2.598	1.3%	2.652	0.7%	2.629	0.2%	2.634	0.0%	2.597	1.4%
21	3.570	0.9%	3.649	3.1%	3.662	3.5%	3.553	0.4%	3.594	1.6%
22	4.431	1.4%	4.586	5.0%	4.753	8.8%	4.394	0.6%	4.416	1.1%

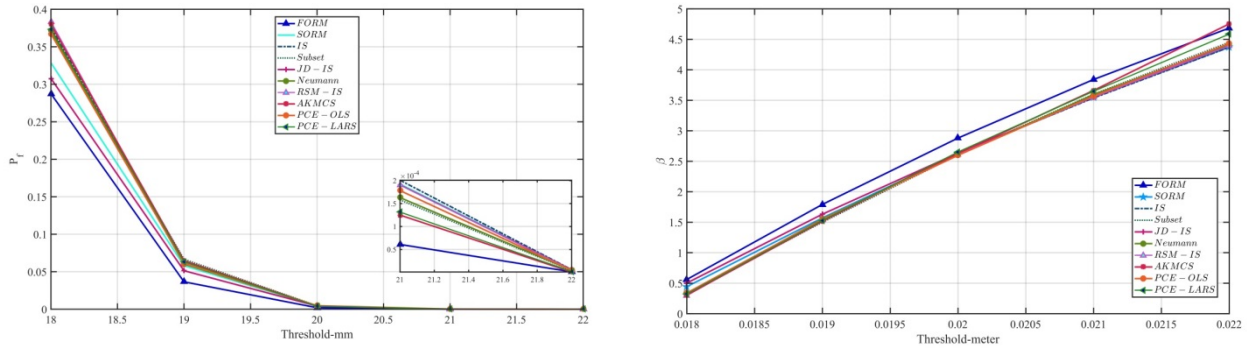

(a) (b)

Figure 4. (a) Influence of the thresholds on the probability of failure, and (b) Influence of the thresholds on the Beta index.

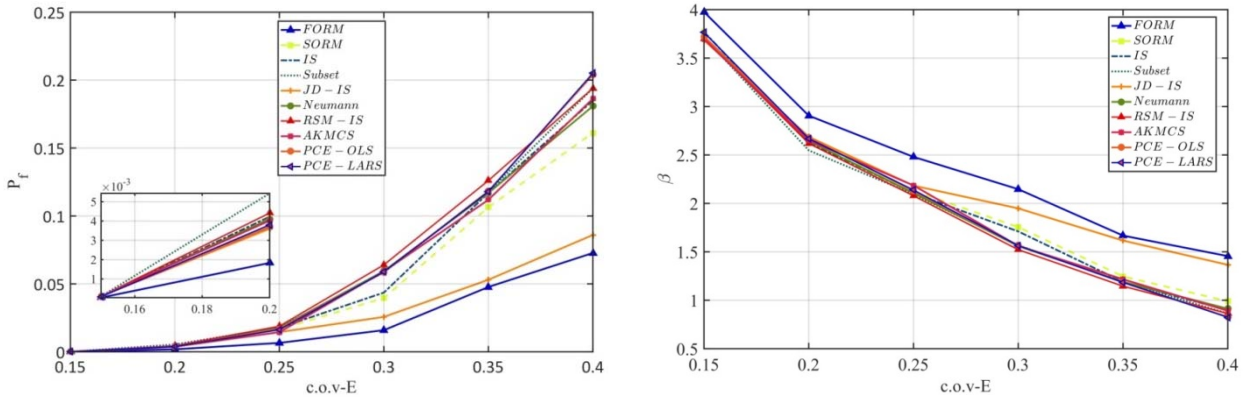

(a) (b)

Figure 5. Estimate of (a) probability of failure, and (b) reliability index in terms of coefficient of variance of the rock evaluated by different reliability methods.

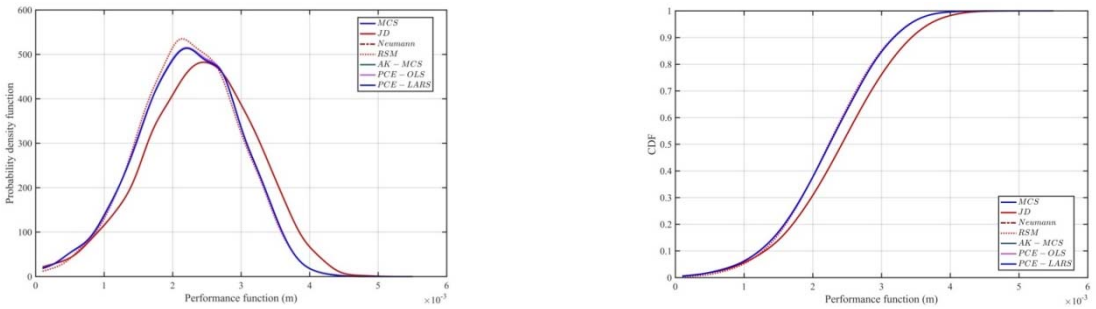

(a) (b)

Figure 6. (a) the probability density functions, and (b) the cumulative distribution functions of the performance function.

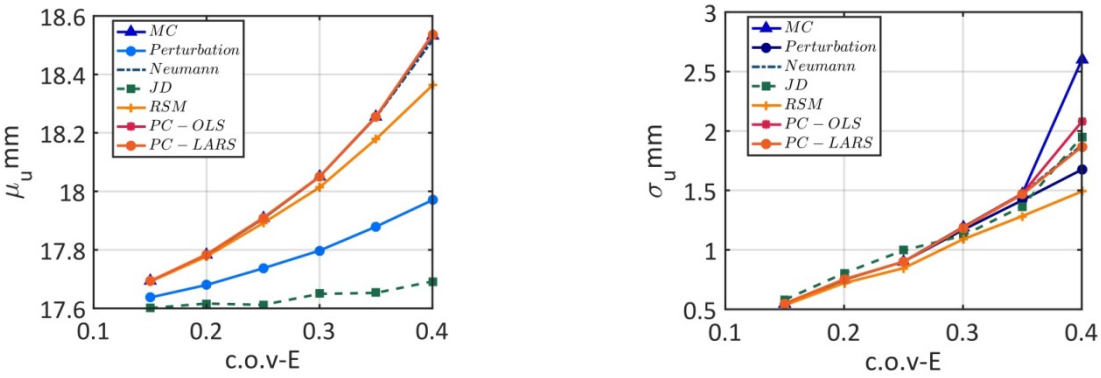

(a) (b)

Figure 7. (a) Mean value, and (b) Standard deviation value of the settlement in terms of coefficient of variance of the rock evaluated by different stochastic methods.

5.3 Sheet pile problem

A sheet pile is studied in this example where the settlement of an elastic soil layer displays spatial variability in its material properties. The uncertainty in the soil material properties is modelled by Gaussian random fields. The site consists of a 5.0 m deep excavation with cantilever sheet piles, without anchors or bottom support (Figure 8a), in a homogeneous soil layer of dense cohesionless sand with uncertain spatially varying mechanical properties. The soil is modelled in 2D with plane-strain finite elements and external loading equal to 10 kPa. It is assumed that the Poisson's ratio of the soil takes a constant value and the only random material property is Young's modulus. The deterministic and probabilistic properties of the sheet pile and soil are shown in Figure 8a and Table 10 respectively. The spatial variability of the soil is modelled by a homogeneous random field, with the following auto-correlation function:

$$\rho(\boldsymbol{\tau}) = \exp(-\frac{\tau_x}{l_x} - \frac{\tau_z}{l_z}) \tag{39}$$

where $\boldsymbol{\tau}$ is the vector of absolute distances in the horizontal and vertical directions, and $l_x = 20m$, $l_z = 5m$ are the correlation length in x, z directions for the Young's modulus E of the soil. The first four terms in the F-K-L representation are considered, resulting in four Gaussian random variables ξ_i. Figure 9b shows a realization of the Gaussian random field representing the uncertainty of Young's modulus.

A refined mesh was first used to get the exact maximum deflection of the sheet pile. Then different meshes were tried in order to design an optimal mesh that meets the 1% error requirement in the maximum deflection. The selected mesh is shown in Figure 8b, which contains 1542 nodes and 1460 elements. The pile is modelled using beam elements with corresponding to a Larssen 24 profile that behaves equally to the sheet pile in bending and axial resistance. The interaction between the sheet pile and the surrounding soil is modelled using

spring elements. The maximum horizontal u_x displacement occurs at the top of the sheet pile. The failure occurs when the value of u_x exceeding a threshold of $u_{max} = 2.5\ cm$, as expressed by the following limit state function:

$$g(\boldsymbol{X}) = u_{max} - u_x \tag{40}$$

Given the random variables $\boldsymbol{X}$ and by using the FEM we can solve the value of u_x.

Table 10 Material properties of the soil in the sheet pile example

Variable	Dist.	Mean kPa	Std kPa	COV
E_{soil}	Normal	50000	15000	0.25

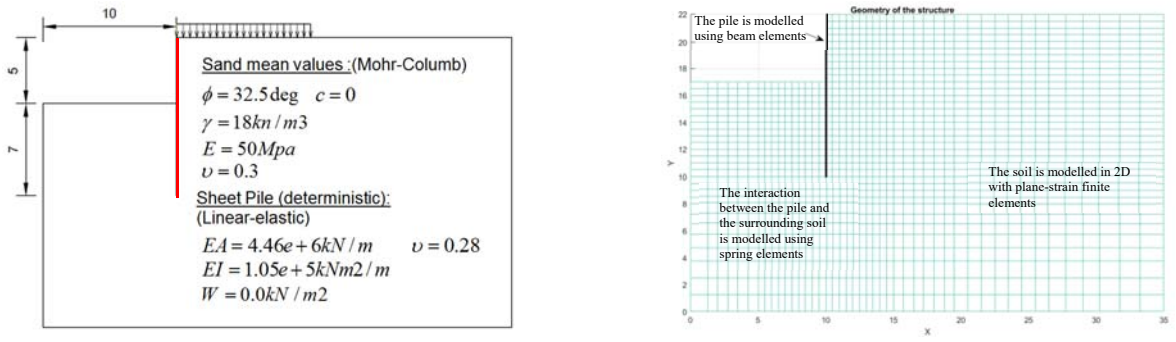

(a) (b)

Figure 8. (a) Sheet pile wall (without anchors). (b) Finite element discretization of the soil.

The mean and standard deviation of the random displacement at the top of the sheet pile is now considered. Figure 9a depicts the deformed shape of the sheet pile and soil computed with the mean value of the random field. The reference value is obtained by LHS with 100,000 model evaluations. The mean and standard deviation for the response reference are 9.86 mm and 3.87 mm respectively. The results obtained using different SRA and SFEM schemes are listed in Table 11, Figures 10a, 10b. It appears that the first order perturbation method estimates acceptable mean only when the variance of the input random field is less than 0.25, while the second order perturbation gives better estimates for the full range of random parameters considered here. The results from the Neumann and PCE methods both give better accuracy than the perturbation methods. As for the efficiency aspect, the intrusive PCE method takes more computational effort than all other methods except MCS. In contrast, the non-intrusive PCE by using the ordinary least regression (OLS) or least angle regression (LARS) and Kriging meta-modelling required less model evaluations.

The probability of failure is investigated by different SRA and SFEM approaches, and the results are summarized in Table 12. The accuracy of each method has been investigated for different variance values of the input random field and plotted in Figure 11. The AK-MCS approach is seen to have the optimal balance between the accuracy in the reliability index and the computational cost, with a relative error of 1% and only 152 finite element runs. FORM runs fastest with the minimum limit state function evaluations, but it gives the worst result in terms of accuracy. The accuracy of the simulation methods (e.g. subset simulation) are better than the FORM and PCE methods, but required a large number of limit state function evaluations to converge with an acceptable level of accuracy. The non-intrusive PCE including both OLS and LARS are also tested here, with the polynomial order set to 4. The random field is discretized with four random variables leading to a total dimensionality of the computational model of 70 (i.e. the number of basis). The experimental design using LHS consists of $N = 157{,}123$ samples for OLS and LARS respectively. The accuracy of the PC expansion for this problem is low compared with the reference value. This is because the probability of failure for this problem is very small and as alluded in the previous examples that the PCE can be used in one-shot for not too small probabilities of failures. Moreover, the computation time may, however, blow up when more than a couple of random variables are used to discretize the random field.

After collecting all the results, it clarifies that the AK-MCS method is the most attractive for problems involving random field because it is accurate with reasonable computational cost even for large coefficients of variation of the input. SORM is the second good method for the reliability index evaluation. The PCE approach also gives accurate results when applied at third and higher orders. The computation time may however blow up when more than 2 or 3 random variables are used to discretize the random field. In contrast, using intrusive polynomial chaos in this context requires increasing the order of expansion, leading rapidly to intractable calculations.

Table 11 Comparison of moment analysis for sheet pile example.

Method	μ_U cm	σ_U cm	Function calls	Time (sec)	Notes
MCS	0.986	0.387	100,000	105,830	LHS
Intrusive PC -Galerkin	1.44	0.93	-	10,772	F-K-L with 4 Rv. p=4
Non-intrusive PCE – OLS	0.985	0.39	157	514	p=4
Non-intrusive PCE – LARS	0.984	0.39	123	150.7	p=4
Perturbation I	0.973	0.82	-	37	F-K-L with 4 Rv.
MCS-Neumann-Lambda	0.983	0.38	-	90	-

Table 12 Comparison of reliability approximations for sheet pile example (Continue).

Method	$P_f \times 10^{-3}$	β	Function calls	Time (sec)	Notes	Relative error ε_β %
FORM	1.1805	3.0406	118	255	-	4.11
SORM (Curvature Fitting method)	1.7936	2.9123	180	502	Improved Breitung	0.29
SORM (Curvature Fitting method)	1.7004	2.9289	180	502	Breitung	0.28
IS	1.7464	2.9207	67518	50145	$cov_{P_f} = 0.01$	-
Subset Simulation	1.9400	2.8878	2778	20596	$cov_{P_f} = 0.22$	1.23
Neumann Expansion	Not converged					
MCS with Neumann-Lambda	1.400	3.0141	-	7811	$cov_{P_f} = 0.01$	3.19
Intrusive PCE (Galerkin)	Required high capacity					
PCE – Quadrature (Smolyak)	array exceeds maximum array size					
PCE – OLS	1.9207	2.8909	157	593	$p = 4$	1.02
PCE – LARS	1.9012	2.8941	123	397	$p = 4$	0.91
AK-MCS	1.8900	2.8959	152	238	$cov_{P_f} = 0.07$	0.85

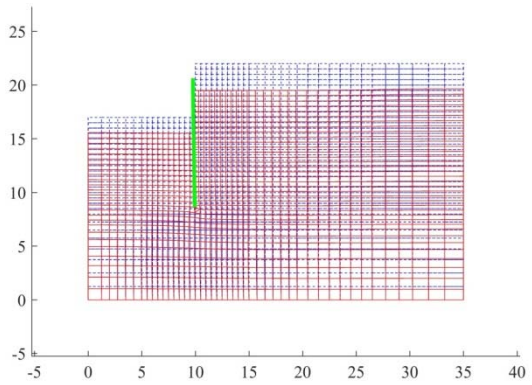

(a)

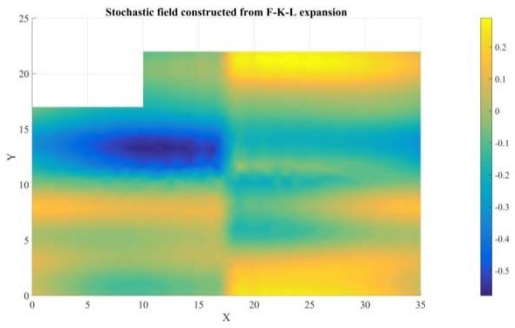

(b)

Figure 9. (a) Deformed shape of the Structure, and (b) Realization of a homogeneous anisotropic normal random field representing the Young's modulus E of the soil.

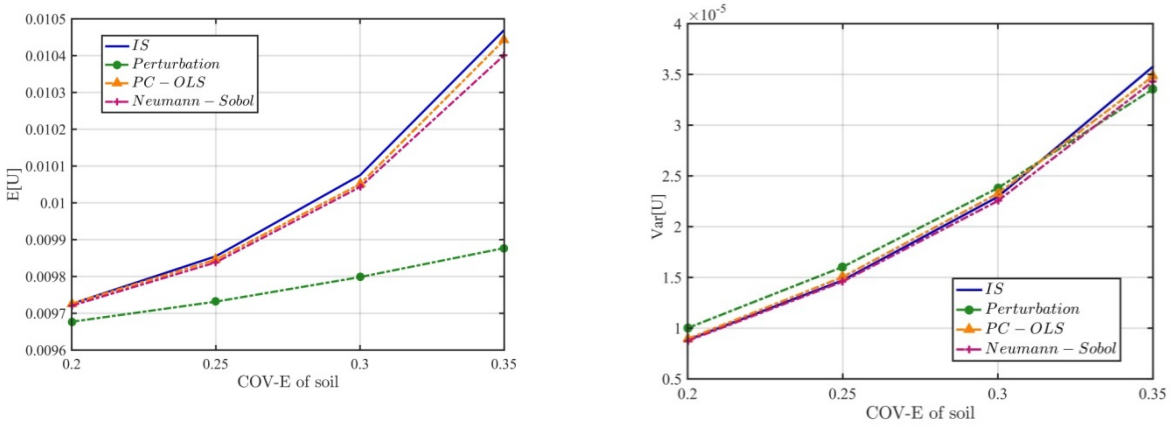

(a) (b)

Figure 10. Estimate of (a) expected value, and (b) variance value of the displacement of sheet pile in terms of coefficient of variance of the soil evaluated by the IS, Perturbation, PC and Neumann method.

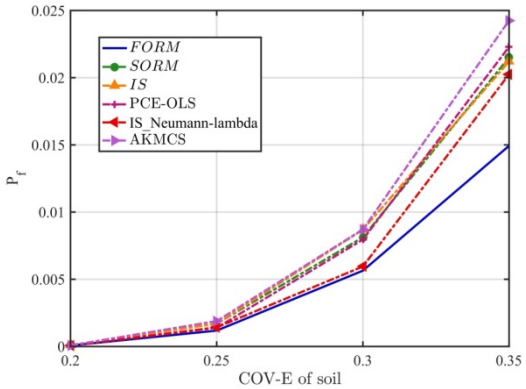

Figure 11. Estimate of probability of failure in terms of coefficient of variance of the soil evaluated by different reliability methods (sheet pile example).

5.4 Frame structure

A three-span, five-story frame structure subjected to horizontal loads is considered in this example, as shown in Figure 12. Three applied loads, two Young's modulus, eight moments of inertia and eight cross-section areas of the frame components are modelled by random variables. There are in total $M = 21$ random variables, denoted by $\boldsymbol{X} = \{P_1, P_2, P_3, E_4, \dots, I_6, \dots, A_{14}, \dots, A_{21}\}^T$. The applied loads and the material properties are assumed respectively to follow a lognormal distribution and truncated Gaussian distribution over $[0, +\infty)$. It is noted that the Gaussian random variables have been truncated in order to avoid non-physical negative realizations. Moreover, the various input random variables are correlated (see [154] for the complete description). The response of interest is the horizontal displacement u at the top right corner of the top floor, with the horizontal loads acting at individual floor levels. The model response can be eventually recast as a function of independent standard Gaussian random variables ξ_i by using Nataf transformation so that it may be expanded onto a PCE made of normalized Hermite polynomials. Of interest are the mean and the standard

deviation of the random maximal displacement $\boldsymbol{U} = \boldsymbol{M}(\boldsymbol{Z}(\boldsymbol{X}))$. The reference value for this example is obtained with the quadrature scheme with a two digit accuracy (15179 model valuations are performed). The reference mean and standard deviation value for the deflection are 0.069 ft. and 0.021 ft, respectively. The statistical moments estimated with different methods are listed in Table 13.

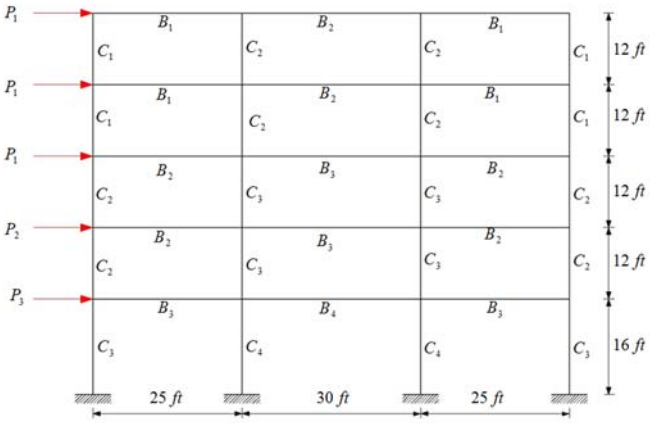

Figure 12. Three-span, five-story frame structure subjected to lateral loads.

Table 13 Comparison of Moment Analysis for Frame structure example.

Method	μ_U ft	σ_U ft	Function calls	Time (sec)	Notes
MCS	0.0652	0.0202	100000		LHS
MCS with Neumann-Lambda	0.0662	0.0202	1000	3.1	LHS
Non-intrusive PCE – OLS (Full PC)	0.0653	0.0200	330	3.5	$p = 2$; $J_{max} = 2$
Non-intrusive PCE – LARS (Sparse PC)	0.0649	0.0200	120	0.48	LOO=0.011

The maximum degree p_{max} of the spars PC is set equal to 7, its target approximation error to 10^{-2}, its maximum interaction order j_{max} to 2, and the cut-off values $\varepsilon_1, \varepsilon_2$ to 5×10^{-5}. The LHS design is used to generate collocation points to calculate PCE coefficients and LARS coefficients, and the experimental design points are enriched until the regression problem is well-posed. An initial sampling of the size $N = M + 1 = 22$ is used. The LARS approximation leads to gain factor of 2.75 (120 finite element runs instead of 330). The expectation and variance value of the deflection for the frame evaluated by different values for the coefficient of variance of material $cov(E_4)$ are presented in Figures 13a and 13b. The perturbation method gives poor results especially when increasing $cov(E_4)$, while all other methods give accurate results compared with MCS. Figure 14 presents the probability density function for the response, which shows a good agreement with the MCS.

A reliability analysis is carried out with respect to the limit state function $g(\boldsymbol{X}) = u_{max} - u_1(\boldsymbol{X})$, where $u_1(\boldsymbol{X})$ is the horizontal component of the top displacement and u_{max} is a given threshold set to 0.2 ft. The reference value of the failure probability P_f is obtained by MCS by using (1,000,000) model frame evaluations to get a coefficient of variation less than 0.05 on P_f. Estimates of the probability of failure and reliability index are calculated by different methods, and the results are summarized in Table 14. It can be observed that FORM requires 209 function evaluations (frame analysis) with approximations yield relative error on β equal to 11 %, while SORM requires 680 function evaluations and give more accurate result than FORM. The results of failure probability analysed with different methods are plotted in Figures 15, 16a and 16b. It can be observed that all methods except for FORM give reasonable results. Furthermore, using $N = 24159$ samples to construct the kernel sampling density, the importance sampling simulation results give an estimate of the probability of failure with the approximated error on β equal to 5%. While the probability of failure $P_f = 2.0575 \times 10^{-4}$, which was obtained by DS using 10,000 directions, gives about 4% approximation error. Nevertheless, other commonly used reliability methods, such as SS over predict the failure probability by 0.6% compared with MCS by using five subsets but with high computation effort. Due to the very slow convergence of the Neumann series, we used only the MCS-Neumann with Lambda parameter, which leads to a

significantly more accurate solution than conventional Neumann with smaller effort. Also, estimates of the failure probability are computed by post-processing a full third order PC (OLS) as well as sparse PC (LARS) approximation. The latter is built up by setting the target approximation error equal to 10^{-3} (this is an overall mean square error that drives the convergence of the adaptive PC expansion). From the result, it can be note that both PCE approximations yield relative errors on β less than 9%. Additionally, we can observe that LARS to be efficient since it makes use of only $N = 700$ runs of the finite element model. In comparison, using a full third order PC expansion would require performance more than $\binom{M+p}{p} = \binom{21+3}{3} = 2024$ and would thus require about $2P \approx 4048$ finite element runs in order to get accurate results. Hence a computational cost multiplied by 5.7 compare to the LARS approach. It is also seen that PCE in the least square sense provides an approximation whose accuracy is controlled globally. In the tail of the distribution of the performance function, it does not guarantee a perfect control of the accuracy. This frame structure has been treated a sparse polynomial chaos of maximum degree 6 was necessary to obtain accurate enough results on the performance function. However, this approach should not be used for very small probabilities less than $P_f = 10^{-4}$. In such a case, it should be better to use other kinds of meta-models to ensure the accuracy. The AK-MCS can approximate the probability of failure with accuracy similar to an MCS with high efficiency. This example shows that AK-MCS can be applied on moderate dimension problems with great effectiveness. For the MPP-based univariate method with numerical integration and the univariate method with simulation [164], the linear approximation of the limit state function in rotated Gaussian space $g_N(v_N)$ was employed. Both versions of the univariate methods provide more accurate results than FORM and SORM with slightly more expensive computational effort, but significantly more efficient than simulation methods. The probability of failure is also evaluated by the full factorial moment method. The results show that it leads to accurate results but with large number of computational model runs.

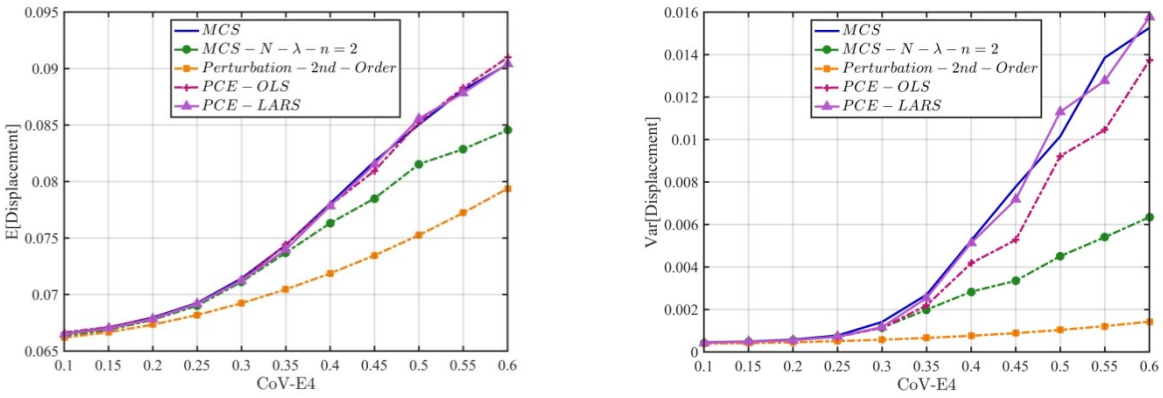

(a) (b)

Figure 13. (a) Expected value, and (b) Variance value of the response evaluated with different value of the coefficient of variance of the Young's modulus of the material E_4

Table 14 Comparison of reliability approximations for Frame structure example.

Method	$P_f = 10^{-4}$	β	Function calls	Time (sec)	Notes	Relative error ε_β %
FORM	0.7846	3.7800	209	10	-	11.62
SORM (Curvature Fitting method)	1.3930	3.6344	252	11.4	Improved Breitung	7.32
SORM (Curvature Fitting method)	1.3396	3.6445	252	11.4	Breitung	7.61
SORM (Point Fitting method)	1.3823	3.6364	680	31	Improved Breitung	7.38
SORM (Point Fitting method)	1.3396	3.6445	680	31	Breitung	7.62
MCS	3.5400	3.3865	1000000	43936	$cov_{P_f} = 0.05$	-

IS	1.7698	3.5722	24159	31	$cov_{P_f} = 0.05$	5.48
DS	2.0575	3.5326	51309	2323	$cov_{P_f} = 0.27$	4.31
Subset Simulation	3.2720	3.4080	212960	9548	$cov_{P_f} = 0.04$	0.63
RSM (second order without cross term)	2.2344	3.5107	731	--	-	3.67
Neumann Expansion	---	---	---	---	Not converged	
MCS with Neumann-Lambda	1.3762	3.6375	9782	28	$cov_{P_f} = 0.025$	7.41
Non-intrusive PCE – OLS	1.4555	3.6231	4048	39	$p = 3$	6.98
Non-intrusive PCE – LARS	1.1059	3.6935	700	23	$p = 3$	9.06
AK-MCS	3.1400	3.4192	142	18.4	$cov_{P_f} = 0.056$	0.97
Moment method (FFMM)	3.7340	3.3718	600	26.4	-	0.43
UDR	3.6280	3.3797	600	26.4	-	0.2

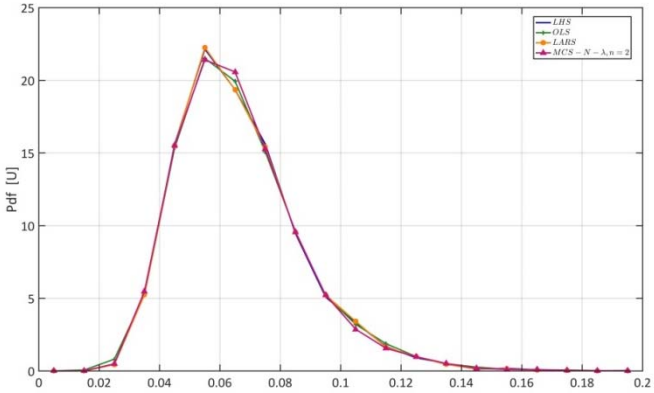

Figure 14. Probability density functions for the response (Frame structure).

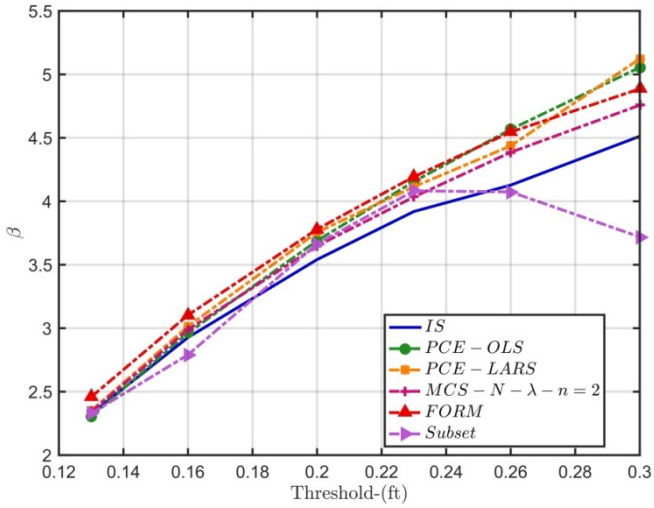

Figure 15. Influence of the threshold on the reliability index (Frame structure).

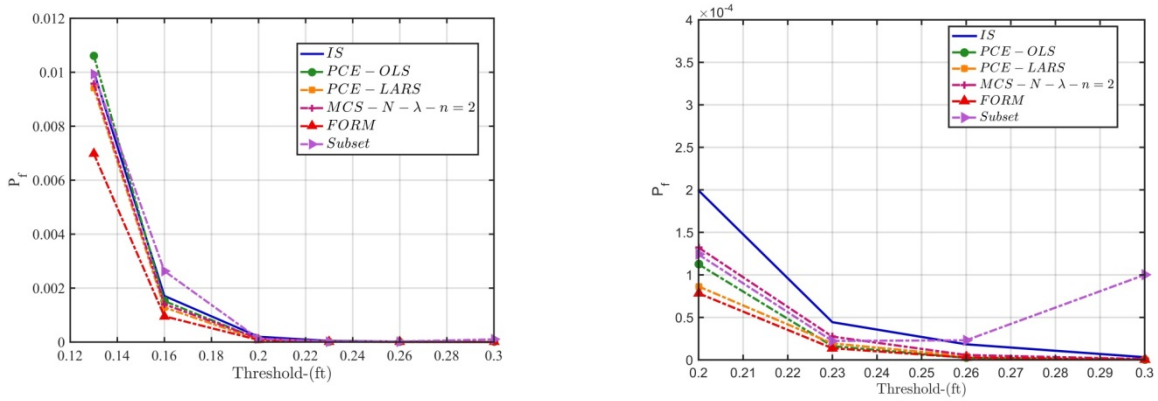

(a) (b)

Figure 16. (a) Influence of the threshold on the probability of failure, and (b) Distribution tail for probability of failure.

6 Conclusion

A comprehensive review and rigorous study of structural reliability analysis and stochastic finite element methods have been completed. The accuracy, efficiency and robustness of each method are analysed in detail against the common set of representative examples, including explicit limit-state functions, geotechnical and structural problems etc. The results from the comparative study provide comprehensive evidence-based references for the performance of different SRA and SFEM approaches. The main concluding remarks are summarised below:

- As the most ancient SRA methods, the theory and computational framework of FORM and SORM are well established in their own context. However, both schemes have severe drawbacks when dealing with practical structures whose limit-state functions can be implicitly defined, non-smooth, of high randomness dimensionality and with large degrees of freedoms.
- The simulation methods have become increasingly attractive in recent years due to the availability of cheaper and fast computers. The main drawback is its high computational cost, especially when dealing with rare events. A number of numerical techniques have been developed to reduce the cost, including IS, LHS, DS and SS methods etc.
- The RSM offers a vehicle to efficiently combine the powerful FEMs with reliability related problems. Methods have also been developed to rationally reduce the size of the probabilistic models using importance measures.
- The SFEM enables the treatment of spatially varying stochastic structural heterogeneity. This is of essential importance, for instance, in the treatment of geotechnical problems, structural problems involving high-frequency vibrations and in problems of elastic stability.
- In the context of intrusive SFEM, a number of algorithms have been developed, including the perturbation, Neumann expansion, JD, and PCE methods etc. The advantages and drawbacks of each method are presented in Table 15.
- The surrogate model based structural reliability analysis has become quite popular in the literature. It is most suitable for cases where the performance function has implicit form and needs to be evaluated point-wise by numerical methods such as FEM. However, most surrogate models suffer from the number of unknown coefficients increasing quickly with the increase in the number of variables (the curse of dimensionality) and selection of the experimental points to construct the surrogate model.
- The meta-models that are used in this paper are PCE (OLS and LARS algorithms), Kriging meta-model, and the combined PCK technique. PCE is a regression technique that models well the global behaviour of the computational model. On the other side, Kriging is known to model well local variations because of its interpolation properties. In fact, PCK is a special case of universal Kriging models where the trend is modelled by orthogonal polynomials. From the comparative study, it is observed that accuracy increases by using PCK instead of the traditional meta-modelling techniques.

- The meta-models are used to compute rare events, such as small failure probabilities by a popular strategy like PCE-IS, AK-MCS, APCK-MCS. In the shown applications, the results of AK-MCS are almost better than that from PCE-IS. But at the same time, these results have large relative errors. Also, APCK-MCS provides an accurate estimation of the statistics of interest for a reasonable amount of runs of the computational model.

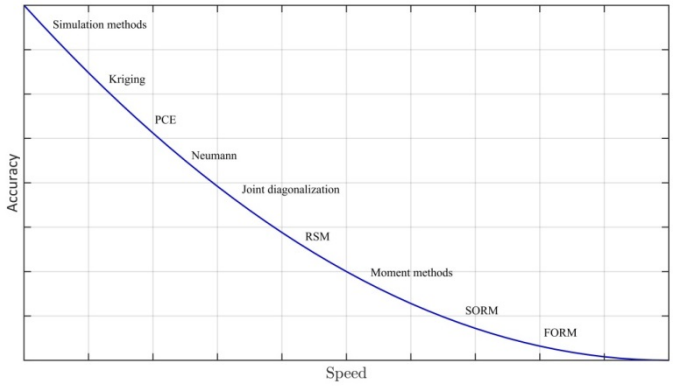

Figure 17. The accuracy via the efficiency for the structural reliability methods.

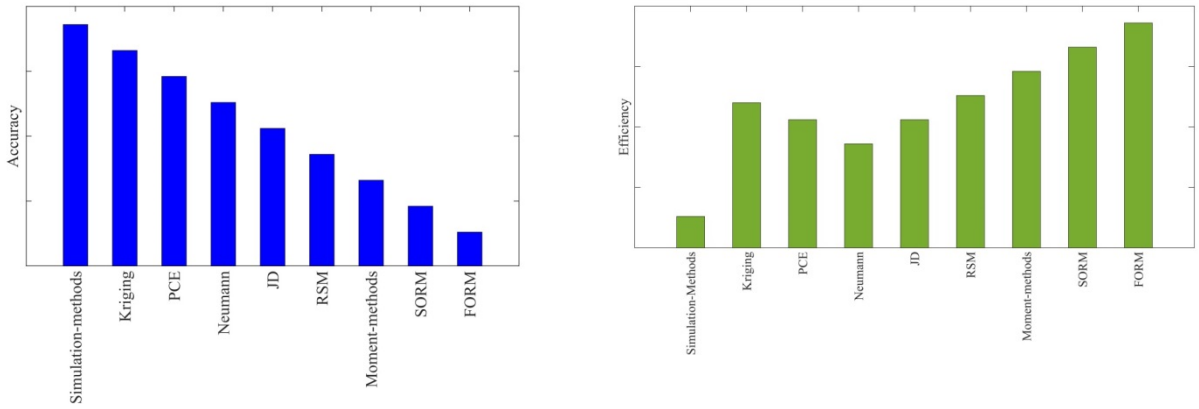

(a) (b)

Figure 18. Bar chart of (a) the accuracy, and (b) the efficiency for the structural reliability methods.

Table 15 Advantage and disadvantage of the reliability methods.

Method	Advantage	Disadvantage
FORM	➢ Efficiency, effectiveness and simplicity when the limit state function is explicitly defined.	➢ The accuracy depends on the shape of the limit state surface, and can only be assessed through comparison with MCS. ➢ Convergence issues when the LSF is nonlinear and/or in the presence of non-Gaussian random variables also for LSF with multiple MPP. ➢ It is not suitable for the LSF which is implicitly defined. ➢ Requires the solution of an optimization problem to find the smallest distance to the limit state. ➢ It requires search MPP. No guarantee to determine the correct MPP.

SORM	➢ More accurate than FORM. ➢ More efficient compared with simulation methods.	➢ Computational efficiency is no greater than that of MCS when the number of random variables is large (~100) [165]. ➢ The accuracy depends on the shape of the failure surface and can only be assessed in comparison with MCS. ➢ It is not particularly suitable for the implicitly defined limit state function. ➢ It depends on FORM's result.
MCS	➢ MCS is very robust in the sense that it can handle complex limit states. ➢ MCS are simple, flexible, friendly to parallel computing, and not restricted by the number of random variables.	➢ High computational cost especially for small probability values.
IS	➢ It is designed to reduce the variance of the Monte Carlo estimators for a given sample size. ➢ IS algorithm is more efficient than Monte Carlo simulation and directional simulation. ➢ It is able to simulate more rare random events.	➢ It requires information about the location of the limit state(s), especially the part closest to the origin in U-space, to be useful. ➢ It faces difficulties when applied to high-dimension problems and when the limit state function has multiple MPPs.
DS	➢ It is relatively efficient compared to MCS.	➢ The accuracy drops drastically when the performance function is highly nonlinear unless the number of sampling directions is large.
SS	➢ It has been capable to solve very complex problems (complex non-linear limit state function in high dimensions) [166]. ➢ It is relatively efficient compared to other simulation methods.	➢ It is capable to reduce the computational efforts needed by MCS by one to two orders of magnitudes; the needed sample size is still essential that is the drawback of its generality.
RSM	➢ It gives comparable results from other computationally more demanding approach. ➢ Identifying the sensitive parameters involved in controlling the system response and helps in quality control measures. ➢ Reduces the number of runs. ➢ Simplified relationship that can be used for practical engineering purposes.	➢ It can sometimes lead to false MPP, and there is no guarantee that the fitted surface is in fact a sufficiently close fit in all regions of interest. ➢ The training points for the construction of RSM model are empirically selected.
Neumann	➢ It is a simple formulation.	➢ The computational efficiency of the method depends on the range of random fluctuations. The fluctuation range allowed by the Neumann expansion method is generally higher than the perturbation methods. ➢ Not suitable for problems with large random variations. ➢ The convergence is very slow.
Perturbation	➢ Only the first two moments of random variables need to be known.	➢ It is restricted to small variability, and the accuracy decreases when the random fluctuation increases.
JD	➢ This method is not sensitive to the number of random variables in the system. ➢ It is better and more accurate than Neumann expansion and perturbation method.	➢ There has not been a mathematically rigorous proof for its accuracy. ➢ It is used with the random field problem and inapplicable with the random variable problems.
Intrusive PCE	➢ Compared with the MCS, the computational cost of gPC is significantly lower. ➢ The computation is efficient and robust. ➢ The use of sampling is not required.	➢ Intrusive methods have the inconveniency of requiring full re-programming of conventional finite element software.

		➢ Their low efficiency, because the simulation runs increase exponentially with the number of random variables and the order of the polynomials used. ➢ The amount of computation required for a given problem is much greater than that of the equivalent deterministic problem.
Collocation method (non-intrusive)	➢ The low number of simulation runs, when few random parameters are involved. ➢ Easy to implement with analysis codes treated as black boxes ➢ Sparse grids reduce the "curse of dimensionality" drastically. ➢ When the same random variable occurs in many different problems, it is sufficient to calculate the integration point set once and to save it for further use.	➢ Less rigorous and their accuracy is poorer than the full projection methods using the Galerkin approach.
AK-MCS	➢ It is independent from the type of the response surface function to be fitted. Also it is not greatly affected by the choice of the space. ➢ Kriging meta-model is more efficient than the other meta-models found in literature	➢ The parameters of the Kriging method significantly affect the reliability results. However, there is no guidance how to select appropriate values for the parameters. ➢ Some parameters used in Kriging are determined by optimization approach. These causes no guarantee a good result for the structural reliability problems.
Classical Moment methods	➢ The probability of failure can be computed, even when the CDFs or PDFs of random variables are unknown. ➢ It is simple and efficiency, while it requires neither iteration nor the computation of derivatives.	➢ The expression of the fourth moment reliability index is too complicated for the engineering use. ➢ It is more suitable for a negative skewness than for a positive value. ➢ It is often considered more suitable for high probability problems. However, at probability levels less than 10^{-5}, P_f deduced by the Pearson system might not be reliable. ➢ If used the third polynomial (cubic) normal distribution to predict the probability, the moment method becomes generally inapplicable to a limit-state function with more than third power random variables. ➢ Two error sources exist: estimating four statistical moments and approximating the response PDF or CDF based on the four actual moments.
Improved Moment method-FFMM	➢ It shows very robust performance in terms of accuracy against the non-normality of inputs.	➢ It suffers from the exponentially increasing number of nodes with random input dimensions, and it seems suitable only for problems with very small dimensionality because of the "curse of dimensionality".
Improved Moment method-UDR	➢ Easy to implement and use.	➢ It is also noted that the accuracy of UDR deteriorates as the interaction effect increases and the high-order moments (skewness and kurtosis) are more vulnerable to this error than low-order moments. ➢ It may be not be adequate for a system with a large number of random variables or strong nonlinearity due to the high-dimensional integrals retained in the residue error of this method.

Acknowledgment

The authors would like to thank the support from the Ministry of Higher Education and Scientific Research in Iraq, the Sêr Cymru National Research Network in Advanced Engineering and Materials, the China Scholarship Council, and the Royal Academy of Engineering.

References

[1] Sudret, B., M. Berveiller, and M. Lemaire, A stochastic finite element method in linear mechanics. *Comptes Rendus Mecanique*, 2004. 332(7): p. 531-537.

[2] B. SUDRET, A.D., Stochastic Finite Element Methods and Reliability-A State-of-the-Art Report, 2000.

[3] Hohenbichler, M. and R. Rackwitz, Non-Normal Dependent Vectors in Structural Safety. *Journal of the Engineering Mechanics Division-Asce*, 1981. 107(6): p. 1227-1238.

[4] Kiureghian, A.D. and P.L. Liu, Structural Reliability under Incomplete Probability Information. *Journal of Engineering Mechanics-Asce*, 1986. 112(1): p. 85-104.

[5] Ghanem, R.G. and P.D. Spanos, Spectral Stochastic Finite-Element Formulation for Reliability-Analysis. *Journal of Engineering Mechanics-Asce*, 1991. 117(10): p. 2351-2372.

[6] Spanos, P.D. and R. Ghanem, Stochastic Finite-Element Expansion for Random-Media. *Journal of Engineering Mechanics-Asce*, 1989. 115(5): p. 1035-1053.

[7] Ghanem, R., Probabilistic characterization of transport in heterogeneous media. *Computer Methods in Applied Mechanics and Engineering*, 1998. 158(3-4): p. 199-220.

[8] Stefanou, G., The stochastic finite element method: Past, present and future. *Computer Methods in Applied Mechanics and Engineering*, 2009. 198(9-12): p. 1031-1051.

[9] Phoon, K.K., S.P. Huang, and S.T. Quek, Implementation of Karhunen-Loeve expansion for simulation using a wavelet-Galerkin scheme. *Probabilistic Engineering Mechanics*, 2002. 17(3): p. 293-303.

[10] Schwab, C. and R.A. Todor, Karhunen-Loeve approximation of random fields by generalized fast multipole methods. *Journal of Computational Physics*, 2006. 217(1): p. 100-122.

[11] Li, C.F., et al., A Fourier-Karhunen-Loeve discretization scheme for stationary random material properties in SFEM. *International Journal for Numerical Methods in Engineering*, 2008. 73(13): p. 1942-1965.

[12] Li, C.F., et al., Fourier representation of random media fields in stochastic finite element modelling. *Engineering Computations*, 2006. 23(7-8): p. 794-817.

[13] Feng, J.W., et al., Statistical reconstruction of two-phase random media. *Computers & Structures*, 2014. 137: p. 78-92.

[14] Feng, J.W., et al., Statistical reconstruction and Karhunen-Loeve expansion for multiphase random media. *International Journal for Numerical Methods in Engineering*, 2016. 105(1): p. 3-32.

[15] Hasofer, A.M. and N.C. Lind, Exact and Invariant Second-Moment Code Format. *Journal of the Engineering Mechanics Division-Asce*, 1974. 100(Nem1): p. 111-121.

[16] Rackwitz, R. and B. Fiessler, Structural Reliability under Combined Random Load Sequences. *Computers & Structures*, 1978. 9(5): p. 489-494.

[17] Lemaire, M., Structural reliability2009, London,Hoboken, NJ: ISTE ; Wiley. 488 p.

[18] Zhang, Y.a.D.K., A.,, Two improved algorithms for reliability analysis, in in R. Rackwitz, G. Augusti, and A. Borr, Editors,1995.

[19] Breitung, K., Asymptotic Approximations for Multinormal Integrals. *Journal of Engineering Mechanics-Asce*, 1984. 110(3): p. 357-366.

[20] Kiureghian, A.D. and M. Destefano, Efficient Algorithm for 2nd-Order Reliability-Analysis. *Journal of Engineering Mechanics-Asce*, 1991. 117(12): p. 2904-2923.

[21] Tvedt, L., Second-order reliability by an exact integral., in Proc., 2nd IFIP Working Conf. on Reliability and Optimization on Struct. Sys.,P., Thoft-Christensen, *Editor* 1988, Springer, New York,. p. 377–384.

[22] Koyluoglu, H.U. and S.R.K. Nielsen, New Approximations for Sorm Integrals. *Structural Safety*, 1994. 13(4): p. 235-246.

[23] Zhao, Y.G. and T. Ono, New approximations for SORM: Part 2. *Journal of Engineering Mechanics-Asce*, 1999. 125(1): p. 86-93.
[24] Adhikari, S., Reliability analysis using parabolic failure surface approximation. *Journal of Engineering Mechanics-Asce*, 2004. 130(12): p. 1407-1427.
[25] Zhang, J.F. and X.P. Du, A Second-Order Reliability Method With First-Order Efficiency. *Journal of Mechanical Design*, 2010. 132(10).
[26] Lee, I., Y. Noh, and D. Yoo, A Novel Second-Order Reliability Method (SORM) Using Noncentral or Generalized Chi-Squared Distributions. *Journal of Mechanical Design*, 2012. 134(10).
[27] Mansour, R. and M. Olsson, A Closed-Form Second-Order Reliability Method Using Noncentral Chi-Squared Distributions. *Journal of Mechanical Design*, 2014. 136(10).
[28] Lu, Z.H., D.Z. Hu, and Y.G. Zhao, Second-Order Fourth-Moment Method for Structural Reliability. *Journal of Engineering Mechanics*, 2017. 143(4).
[29] Feng, Y.T., C.F. Li, and D.R.J. Owen, A directed Monte Carlo solution of linear stochastic algebraic system of equations. *Finite Elements in Analysis and Design*, 2010. 46(6): p. 462-473.
[30] Schueller, G.I. and R. Stix, A Critical-Appraisal of Methods to Determine Failure Probabilities. *Structural Safety*, 1987. 4(4): p. 293-309.
[31] Engelund, S. and R. Rackwitz, A Benchmark Study on Importance Sampling Techniques in Structural Reliability. *Structural Safety*, 1993. 12(4): p. 255-276.
[32] M., B.C.a.M., Time-variant reliability – Computational approaches based on FORM and importance sampling,, 2002, In AMAS Course on Reliability-Based Optimization RBO'02,. p. 9-34.
[33] Ang, G.L., A.H.S. Ang, and W.H. Tang, Optimal Importance-Sampling Density Estimator. *Journal of Engineering Mechanics-Asce*, 1992. 118(6): p. 1146-1163.
[34] Kass, R.E., et al., Markov chain Monte Carlo in practice: A roundtable discussion. *American Statistician*, 1998. 52(2): p. 93-100.
[35] Au, S.K. and J.L. Beck, A new adaptive importance sampling scheme for reliability calculations. *Structural Safety*, 1999. 21(2): p. 135-158.
[36] NN., S., Optimization of entropy under uncertainty., 1995, University of California: San Diego.
[37] Wang, G.S. and A.H.S. Ang, Adaptive Kernel-Method for Evaluating Structural System Reliability. *Structural Safety & Reliability, Vols 1-3*, 1994: p. 1495-1500.
[38] Bucher, C.G., Adaptive Sampling - an Iterative Fast Monte-Carlo Procedure. *Structural Safety*, 1988. 5(2): p. 119-126.
[39] Bjerager, P., Probability Integration by Directional Simulation. *Journal of Engineering Mechanics-Asce*, 1988. 114(8): p. 1285-1302.
[40] Ditlevsen, O., R.E. Melchers, and H. Gluver, General Multidimensional Probability Integration by Directional Simulation. *Computers & Structures*, 1990. 36(2): p. 355-368.
[41] Melchers, R.E., Structural System Reliability Assessment Using Directional Simulation. *Structural Safety*, 1994. 16(1-2): p. 23-37.
[42] Moarefzadeh, M.R. and R.E. Melchers, Directional importance sampling for ill-proportioned spaces. *Structural Safety*, 1999. 21(1): p. 1-22.
[43] Katsuki, S. and D.M. Frangopol, Hyperspace Division Method for Structural Reliability. *Journal of Engineering Mechanics-Asce*, 1994. 120(11): p. 2405-2427.
[44] Nie, J. and B.R. Ellingwood, Directional methods for structural reliability analysis. *Structural Safety*, 2000. 22(3): p. 233-249.
[45] Nie, J.S. and B.R. Ellingwood, Finite element-based structural reliability assessment using efficient directional simulation. *Journal of Engineering Mechanics-Asce*, 2005. 131(3): p. 259-267.
[46] Au, S.K. and J.L. Beck, Estimation of small failure probabilities in high dimensions by subset simulation. *Probabilistic Engineering Mechanics*, 2001. 16(4): p. 263-277.
[47] Au, S.-K. and Y. Wang, Engineering risk assessment with subset simulation2014. 315 pages.
[48] Ching, J., S.K. Au, and J.L. Beck, Reliability estimation for dynamical systems subject to stochastic excitation using subset simulation with splitting. *Computer Methods in Applied Mechanics and Engineering*, 2005. 194(12-16): p. 1557-1579.

[49] Ching, J., J.L. Beck, and S.K. Au, Hybrid Subset Simulation method for reliability estimation of dynamical systems subject to stochastic excitation. *Probabilistic Engineering Mechanics*, 2005. 20(3): p. 199-214.
[50] Katafygiotis, L.S. and S.H. Cheung, Application of spherical subset simulation method and auxiliary domain method on a benchmark reliability study. *Structural Safety*, 2007. 29(3): p. 194-207.
[51] Zuev, K.M. and L.S. Katafygiotis, Modified Metropolis-Hastings algorithm with delayed rejection. *Probabilistic Engineering Mechanics*, 2011. 26(3): p. 405-412.
[52] Au, S.K. and J.L. Beck, Subset simulation and its application to seismic risk based on dynamic analysis. *Journal of Engineering Mechanics*, 2003. 129(8): p. 901-917.
[53] Tee, K.F., L.R. Khan, and H.S. Li, Application of subset simulation in reliability estimation of underground pipelines. *Reliability Engineering & System Safety*, 2014. 130: p. 125-131.
[54] Song, S.F., Z.Z. Lu, and H.W. Qiao, Subset simulation for structural reliability sensitivity analysis. *Reliability Engineering & System Safety*, 2009. 94(2): p. 658-665.
[55] Wang, Y., Z.J. Cao, and S.K. Au, Practical reliability analysis of slope stability by advanced Monte Carlo simulations in a spreadsheet. *Canadian Geotechnical Journal*, 2011. 48(1): p. 162-172.
[56] Wang, B.S., et al., Efficient functional reliability estimation for a passive residual heat removal system with subset simulation based on importance sampling. *Progress in Nuclear Energy*, 2015. 78: p. 36-46.
[57] Mckay, M.D., R.J. Beckman, and W.J. Conover, A Comparison of Three Methods for Selecting Values of Input Variables in the Analysis of Output from a Computer Code. *Technometrics*, 1979. 21(2): p. 239-245.
[58] Iman, R.L. and W.J. Conover, A Distribution-Free Approach to Inducing Rank Correlation among Input Variables. *Communications in Statistics Part B-Simulation and Computation*, 1982. 11(3): p. 311-334.
[59] Stein, M., Large Sample Properties of Simulations Using Latin Hypercube Sampling. *Technometrics*, 1987. 29(2): p. 143-151.
[60] Owen, A.B., Controlling Correlations in Latin Hypercube Samples. *Journal of the American Statistical Association*, 1994. 89(428): p. 1517-1522.
[61] Ziha, K., Descriptive Sampling in Structural Safety. *Structural Safety*, 1995. 17(1): p. 33-41.
[62] Olsson, A.M.J. and G.E. Sandberg, Latin hypercube sampling for stochastic finite element analysis. *Journal of Engineering Mechanics-Asce*, 2002. 128(1): p. 121-125.
[63] Pebesma, E.J. and G.B.M. Heuvelink, Latin hypercube sampling of Gaussian random fields. *Technometrics*, 1999. 41(4): p. 303-312.
[64] Monteiro, R., Sampling based numerical seismic assessment of continuous span RC bridges. *Engineering Structures*, 2016. 118: p. 407-420.
[65] Olsson, A., G. Sandberg, and O. Dahlblom, On Latin hypercube sampling for structural reliability analysis. *Structural Safety*, 2003. 25(1): p. 47-68.
[66] Helton, J.C. and F.J. Davis, Latin hypercube sampling and the propagation of uncertainty in analyses of complex systems. *Reliability Engineering & System Safety*, 2003. 81(1): p. 23-69.
[67] Yu, H., et al., Probabilistic Load Flow Evaluation With Hybrid Latin Hypercube-Sampling and Cholesky Decomposition. *Ieee Transactions on Power Systems*, 2009. 24(2): p. 661-667.
[68] Morokoff, W.J. and R.E. Caflisch, Quasi-Monte Carlo Integration. *Journal of Computational Physics*, 1995. 122(2): p. 218-230.
[69] Faravelli, L., Response-Surface Approach for Reliability-Analysis. *Journal of Engineering Mechanics-Asce*, 1989. 115(12): p. 2763-2781.
[70] Zheng, Y. and P.K. Das, Improved response surface method and its application to stiffened plate reliability analysis. *Engineering Structures*, 2000. 22(5): p. 544-551.
[71] Roussouly, N., F. Petitjean, and M. Salaun, A new adaptive response surface method for reliability analysis. *Probabilistic Engineering Mechanics*, 2013. 32: p. 103-115.
[72] Bucher, C.G. and U. Bourgund, A Fast and Efficient Response-Surface Approach for Structural Reliability Problems. *Structural Safety*, 1990. 7(1): p. 57-66.
[73] Rajashekhar, M.R. and B.R. Ellingwood, A New Look at the Response-Surface Approach for Reliability-Analysis. *Structural Safety*, 1993. 12(3): p. 205-220.

[74] Kim, S.H. and S.W. Na, Response surface method using vector projected sampling points. *Structural Safety*, 1997. 19(1): p. 3-19.
[75] Lee, S.H. and B.M. Kwak, Response surface augmented moment method for efficient reliability analysis. *Structural Safety*, 2006. 28(3): p. 261-272.
[76] Goswami, S., S. Ghosh, and S. Chakraborty, Reliability analysis of structures by iterative improved response surface method. *Structural Safety*, 2016. 60: p. 56-66.
[77] Hadidi, A., B.F. Azar, and A. Rafiee, Efficient response surface method for high-dimensional structural reliability analysis. *Structural Safety*, 2017. 68: p. 15-27.
[78] Gomes, H.M. and A.M. Awruch, Comparison of response surface and neural network with other methods for structural reliability analysis. *Structural Safety*, 2004. 26(1): p. 49-67.
[79] Hurtado, J.E., An examination of methods for approximating implicit limit state functions from the viewpoint of statistical learning theory. *Structural Safety*, 2004. 26(3): p. 271-293.
[80] Dai, H.Z., H. Zhang, and W. Wang, A Multiwavelet Neural Network-Based Response Surface Method for Structural Reliability Analysis. *Computer-Aided Civil and Infrastructure Engineering*, 2015. 30(2): p. 151-162.
[81] Jiang, Y.B., et al., Multiple response surfaces method with advanced classification of samples for structural failure function fitting. *Structural Safety*, 2017. 64: p. 87-97.
[82] G., M., The intrinsic random functions and their applications. *Advances in Applied Probability*, 1973. 5(3): p. 439–68.
[83] Jones, D.R., M. Schonlau, and W.J. Welch, Efficient global optimization of expensive black-box functions. *Journal of Global Optimization*, 1998. 13(4): p. 455-492.
[84] Romero, V.J., L.P. Swiler, and A.A. Giunta, Construction of response surfaces. based on progressive-lattice-sampling experimental designs with application to uncertainty propagation. *Structural Safety*, 2004. 26(2): p. 201-219.
[85] Kaymaz, I., Application of kriging method to structural reliability problems. *Structural Safety*, 2005. 27(2): p. 133-151.
[86] Lophaven SN, N.H., Sondergaard J., DACE, a matlab Kriging toolbox, version 2.0., 2002a., IMM-TR-2002-12: Technical University of Denmark.
[87] Bichon, B.J., et al., Efficient Global Reliability Analysis for Nonlinear Implicit Performance Functions. *Aiaa Journal*, 2008. 46(10): p. 2459-2468.
[88] Echard, B., N. Gayton, and M. Lemaire, AK-MCS: An active learning reliability method combining Kriging and Monte Carlo Simulation. *Structural Safety*, 2011. 33(2): p. 145-154.
[89] Santner, T., B.Williams, andW. Notz, The design and analysis of computer experiments. Springer series in Statistics2003: Springer.
[90] Bachoc, F., Cross Validation and Maximum Likelihood estimations of hyper-parameters of Gaussian processes with model misspecification. *Computational Statistics & Data Analysis*, 2013. 66: p. 55-69.
[91] Schobi, R., B. Sudret, and S. Marelli, Rare event estimation using Polynomial-Chaos-Kriging. *ASCE-ASME Journal of Risk and Uncertainty in Engineering Systems, Part A: Civil Engineering*, 2015.
[92] Dani, V., T. P. Hayes, and S. M. Kakade, Stochastic linear optimization under bandit feedback., in In The 21st Annual Conference on Learning Theory (COLT 2008)2008.
[93] Srinivas, N., et al., Information-Theoretic Regret Bounds for Gaussian Process Optimization in the Bandit Setting. *Ieee Transactions on Information Theory*, 2012. 58(5): p. 3250-3265.
[94] DH., E., An application of numerical integration techniques to statistical tolerancing, III – general distributions. *Technometrics*, 1972. 14: p. 23-35.
[95] Seo, H.S. and B.M. Kwak, Efficient statistical tolerance analysis for general distributions using three-point information. *International Journal of Production Research*, 2002. 40(4): p. 931-944.
[96] Hall, A.R., Generalized Method of Moments.2005, New York:: Oxford University Press.
[97] Rabitz, H. and O.F. Alis, General foundations of high-dimensional model representations. *Journal of Mathematical Chemistry*, 1999. 25(2-3): p. 197-233.
[98] Rahman, S. and H. Xu, A univariate dimension-reduction method for multi-dimensional integration in stochastic mechanics. *Probabilistic Engineering Mechanics*, 2004. 19(4): p. 393-408.
[99] Hong, H.P., Point-estimate moment-based reliability analysis. *Civil Engineering Systems*, 1996. 13(4): p. 281-294.

[100] Zhao, Y.G. and T. Ono, Moment methods for structural reliability. *Structural Safety*, 2001. 23(1): p. 47-75.
[101] Taguchi, G., Performance Analysis Design. *International Journal of Production Research*, 1978. 16(6): p. 521-530.
[102] Derrico, J.R. and N.A. Zaino, Statistical Tolerancing Using a Modification of Taguchi Method. *Technometrics*, 1988. 30(4): p. 397-405.
[103] Zhao, Y.G. and Z.H. Lu, Applicable range of the fourth-moment method for structural reliability. *Journal of Asian Architecture and Building Engineering*, 2007. 6(1): p. 151-158.
[104] Xu, H. and S. Rahman, A generalized dimension-reduction method for multidimensional integration in stochastic mechanics. *International Journal for Numerical Methods in Engineering*, 2004. 61(12): p. 1992-2019.
[105] Li, C.F., Y.T. Feng, and D.R.J. Owen, Explicit solution to the stochastic system of linear algebraic equations (alpha(1)A(1)+alpha(2)A(2)+center dot center dot center dot+alpha(m)A(m)) x = b. *Computer Methods in Applied Mechanics and Engineering*, 2006. 195(44-47): p. 6560-6576.
[106] Liu, W.K., T. Belytschko, and A. Mani, Random Field Finite-Elements. *International Journal for Numerical Methods in Engineering*, 1986. 23(10): p. 1831-1845.
[107] Van den Nieuwenhof, B. and J.P. Coyette, Modal approaches for the stochastic finite element analysis of structures with material and geometric uncertainties. *Computer Methods in Applied Mechanics and Engineering*, 2003. 192(33-34): p. 3705-3729.
[108] Kamiński, M.M., The stochastic perturbation method for computational mechanics. xviii, 330 pages.
[109] Baecher, G.B. and T.S. Ingra, Stochastic Fem in Settlement Predictions. *Journal of the Geotechnical Engineering Division-Asce*, 1981. 107(4): p. 449-463.
[110] Phoon, K.K., et al., Reliability-Analysis of Pile Settlement. *Journal of Geotechnical Engineering-Asce*, 1990. 116(11): p. 1717-1735.
[111] Liu, W.K., T. Belytschko, and A. Mani, Probabilistic Finite-Elements for Nonlinear Structural Dynamics. *Computer Methods in Applied Mechanics and Engineering*, 1986. 56(1): p. 61-81.
[112] Wang, X.Y., et al., A priori error estimation for the stochastic perturbation method. *Computer Methods in Applied Mechanics and Engineering*, 2015. 286: p. 1-21.
[113] Wang, X., S. Cen, and C. Li, Generalized Neumann Expansion and Its Application in Stochastic Finite Element Methods. *Mathematical Problems in Engineering*, 2013. 2013: p. 13.
[114] Shinozuka, M. and G. Deodatis, Response Variability of Stochastic Finite-Element Systems. *Journal of Engineering Mechanics-Asce*, 1988. 114(3): p. 499-519.
[115] Yamazaki, F., M. Shinozuka, and G. Dasgupta, Neumann Expansion for Stochastic Finite-Element Analysis. *Journal of Engineering Mechanics-Asce*, 1988. 114(8): p. 1335-1354.
[116] Araujo, J.M. and A.M. Awruch, On Stochastic Finite-Elements for Structural-Analysis. *Computers & Structures*, 1994. 52(3): p. 461-469.
[117] Chakraborty, S. and S.S. Dey, A stochastic finite element dynamic analysis of structures with uncertain parameters. *International Journal of Mechanical Sciences*, 1998. 40(11): p. 1071-1087.
[118] Wang, X.Y., S. Cen, and C.F. Li, Generalized Neumann Expansion and Its Application in Stochastic Finite Element Methods. *Mathematical Problems in Engineering*, 2013.
[119] Papadrakakis, M. and V. Papadopoulos, Robust and efficient methods for stochastic finite element analysis using Monte Carlo simulation. *Computer Methods in Applied Mechanics and Engineering*, 1996. 134(3-4): p. 325-340.
[120] Avila da, S.C.R. and A.T. Beck, New method for efficient Monte Carlo-Neumann solution of linear stochastic systems. *Probabilistic Engineering Mechanics*, 2015. 40: p. 90-96.
[121] Li, C.F., et al., A joint diagonalisation approach for linear stochastic systems. *Computers & Structures*, 2010. 88(19-20): p. 1137-1148.
[122] Li, C.F., Stochastic Finite Element Modelling of Elementary Random Media, 2006, University of Wales Swansea: UK.
[123] Wan, X.L. and G.E.M. Karniadakis, Multi-element generalized polynomial chaos for arbitrary probability measures. *Siam Journal on Scientific Computing*, 2006. 28(3): p. 901-928.
[124] Xiu, D.B. and G.E. Karniadakis, The Wiener-Askey polynomial chaos for stochastic differential equations. *Siam Journal on Scientific Computing*, 2002. 24(2): p. 619-644.

[125] Xiu, D.B. and G.E. Karniadakis, Modeling uncertainty in flow simulations via generalized polynomial chaos. *Journal of Computational Physics*, 2003. 187(1): p. 137-167.
[126] Rupert, C.P. and C.T. Miller, An analysis of polynomial chaos approximations for modeling single-fluid-phase flow in porous medium systems. *Journal of Computational Physics*, 2007. 226(2): p. 2175-2205.
[127] Lin, G. and G.E. Karniadakis, A discontinuous Galerkin method for two-temperature plasmas. *Computer Methods in Applied Mechanics and Engineering*, 2006. 195(25-28): p. 3504-3527.
[128] Sepahvand, K., S. Marburg, and H.J. Hardtke, Numerical solution of one-dimensional wave equation with stochastic parameters using generalized polynomial chaos expansion. *Journal of Computational Acoustics*, 2007. 15(4): p. 579-593.
[129] Sudret, B. and A.D. Kiureghian, Comparison of finite element reliability methods. *Probabilistic Engineering Mechanics*, 2002. 17(4): p. 337-348.
[130] Ghiocel, D.M. and R.G. Ghanem, Stochastic finite-element analysis of seismic soil-structure interaction. *Journal of Engineering Mechanics-Asce*, 2002. 128(1): p. 66-77.
[131] Sudret, B., M. Lemaire, and M. Lemaire, Application of a stochastic finite element procedure to reliability analysis. *Reliability and Optimization of Structural Systems*, 2004: p. 319-327.
[132] Sudret, B., M. Berveiller, and M. Lemaire, A stochastic finite element procedure for moment and reliability analysis. *Eur. J. Comput. Mech.*, 2006. 15(7-8): p. 825–866.
[133] Foo, J., X.L. Wan, and G.E. Karniadakis, The multi-element probabilistic collocation method (ME-PCM): Error analysis and applications. *Journal of Computational Physics*, 2008. 227(22): p. 9572-9595.
[134] Nobile, F., R. Tempone, and C.G. Webster, An anisotropic sparse grid stochastic collocation method for partial differential equations with random input data. *Siam Journal on Numerical Analysis*, 2008. 46(5): p. 2411-2442.
[135] Ghanem, R.G. and R.M. Kruger, Numerical solution of spectral stochastic finite element systems. *Computer Methods in Applied Mechanics and Engineering*, 1996. 129(3): p. 289-303.
[136] Elman, H.C., et al., Efficient iterative algorithms for the stochastic finite element method with application to acoustic scattering. *Computer Methods in Applied Mechanics and Engineering*, 2005. 194(9-11): p. 1037-1055.
[137] Verhoosel, C.V., M.A. Gutierrez, and S.J. Hulshoff, Iterative solution of the random eigenvalue problem with application to spectral stochastic finite element systems. *International Journal for Numerical Methods in Engineering*, 2006. 68(4): p. 401-424.
[138] Chung, D.B., et al., Efficient numerical strategies for spectral stochastic finite element models. *International Journal for Numerical Methods in Engineering*, 2005. 64(10): p. 1334-1349.
[139] Pellissetti, M.F. and R.G. Ghanem, Iterative solution of systems of linear equations arising in the context of stochastic finite elements. *Advances in Engineering Software*, 2000. 31(8-9): p. 607-616.
[140] Saad, Y. and H.A. van der Vorst, Iterative solution of linear systems in the 20th century. *Journal of Computational and Applied Mathematics*, 2000. 123(1-2): p. 1-33.
[141] Tootkaboni, M., L. Graham-Brady, and B.W. Schafer, Geometrically non-linear behavior of structural systems with random material property: An asymptotic spectral stochastic approach. *Computer Methods in Applied Mechanics and Engineering*, 2009. 198(37-40): p. 3173-3185.
[142] Ngah, M.F. and A. Young, Application of the spectral stochastic finite element method for performance prediction of composite structures. *Composite Structures*, 2007. 78(3): p. 447-456.
[143] Baroth, J., et al., An efficient SFE method using Lagrarge polynomials: Application to nonlinear mechanical problems with uncertain parameters. *Computer Methods in Applied Mechanics and Engineering*, 2007. 196(45-48): p. 4419-4429.
[144] Bressolette, P., M. Fogli, and C. Chauviere, A stochastic collocation method for large classes of mechanical problems with uncertain parameters. *Probabilistic Engineering Mechanics*, 2010. 25(2): p. 255-270.
[145] SA., S., Quadrature and interpolation formulas for tensor products of certain classes of functions. *Soviet Math Dokl*, 1963. 4: p. 240-243.
[146] Gerstner, T. and M. Griebel, Numerical integration using sparse grids. *Numerical Algorithms*, 1998. 18(3-4): p. 209-232.

[147] Barthelmann, V., E. Novak, and K. Ritter, High dimensional polynomial interpolation on sparse grids. *Advances in Computational Mathematics*, 2000. 12(4): p. 273-288.
[148] Sudret, B., G. Blatman, and M. Berveiller, Quasi random numbers in stochastic finite element analysis - application to global sensitivity analysis. *Applications of Statisics and Probability in Civil Engineering*, 2007: p. 257-258.
[149] Niederreiter, H., Random number generation and quasi-Monte Carlo methods. CBMS-NSF regional conference series in applied mathematics1992, Philadelphia, Pa.: Society for Industrial and Applied Mathematics. vi, 241 p.
[150] Blatman, G. and B. Sudret, Sparse polynomial chaos expansions and adaptive stochastic finite elements using a regression approach. *Comptes Rendus Mecanique*, 2008. 336(6): p. 518-523.
[151] Isukapalli, S.S., Uncertainty Analysis of Transport-Transformation Models, 1999, The State University of New Jersey.
[152] Berveiller, M., Stochastic finite elements: intrusive and non intrusive methods for reliability analysis., 2005, Université Blaise Pascal: Clermont-Ferrand.
[153] Sudret, B., Global sensitivity analysis using polynomial chaos expansions. *Reliability Engineering & System Safety*, 2008. 93(7): p. 964-979.
[154] Blatman, G. and B. Sudret, An adaptive algorithm to build up sparse polynomial chaos expansions for stochastic finite element analysis. *Probabilistic Engineering Mechanics*, 2010. 25(2): p. 183-197.
[155] Allen, C.D., The prediction sum of squares as a criterion for selecting prediction variables., T.R. 23, *Editor* 1971, Dept. of Statistics: University of Kentucky.
[156] Blatman, G., Adaptive sparse polynomial chaos expansions for uncertainty propagation and sensitivity analysis, 2009, Universit´e Blaise Pascal: Clermont-Ferrand.
[157] Blatman, G. and B. Sudret, Adaptive sparse polynomial chaos expansion based on least angle regression. *Journal of Computational Physics*, 2011a. 230(6): p. 2345-2367.
[158] Blatman, G. and B. Sudret, Principal component analysis and Least Angle Regression in spectral stochastic finite element analysis. *Applications of Statistics and Probability in Civil Engineering*, 2011b: p. 669-676.
[159] Yadav, V. and S. Rahman, Adaptive-sparse polynomial dimensional decomposition methods for high-dimensional stochastic computing. *Computer Methods in Applied Mechanics and Engineering*, 2014. 274: p. 56-83.
[160] Lee, S.H. and W. Chen, A comparative study of uncertainty propagation methods for black-box-type problems. *Structural and Multidisciplinary Optimization*, 2009. 37(3): p. 239-253.
[161] Kersaudy, P., et al., A new surrogate modeling technique combining Kriging and polynomial chaos expansions - Application to uncertainty analysis in computational dosimetry. *Journal of Computational Physics*, 2015. 286: p. 103-117.
[162] Kiureghian, A.D., H.Z. Lin, and S.J. Hwang, 2nd-Order Reliability Approximations. *Journal of Engineering Mechanics-Asce*, 1987. 113(8): p. 1208-1225.
[163] Borri, A. and E. Speranzini, Structural reliability analysis using a standard deterministic finite element code. *Structural Safety*, 1997. 19(4): p. 361-382.
[164] Rahman, S. and D. Wei, A univariate approximation at most probable point for higher-order reliability analysis. *International Journal of Solids and Structures*, 2006. 43(9): p. 2820-2839.
[165] Skaggs, T.H. and D.A. Barry, Assessing uncertainty in subsurface solute transport: Efficient first-order reliability methods. *Environmental Software*, 1996. 11(1-3): p. 179-184.
[166] Pradlwarter, H.J. and G.I. Schueller, Reliability of deterministic non-linear systems subjected to stochastic dynamic excitation. *International Journal for Numerical Methods in Engineering*, 2011. 85(9): p. 1160-1176.